



**Politecnico
di Torino**

Politecnico di Torino

Master Degree Course in Electronics
Engineering (Radio Frequency Design)

Master Degree Thesis

**LOW POWER RADIO FREQUENCY
COMMUNICATION SYSTEM FOR BIOMEDICAL
APPLICATION**

Supervisor:

Prof. Ladislau Matekovits

Candidate:

Amir Kamal Eddine

Matricola: 258359

Academic Year 2021-2022

DEDICATION

This thesis is dedicated to the people who have supported me throughout my education: my parents, my family members and my close friends.

Special thanks to my supervisor, Professor Ladislau Matekovits to his support, guidance and supervision during my master's degree thesis.

ACKNOWLEDGMENTS

The completion of this undertaking could not have been possible without the participation and assistance of many people. I would like to express my deep appreciation particularly:

To my parents who did their roles even if they were not in good terms for almost three years.

To my supervisor, Professor Ladislau Matekovits, for his endless support during my Master's degree thesis.

To professors Mohammad Taki, Ali Assi, Hussein Kassem and Ali Hallal for their kind and understanding spirit during my Bachelor Degree.

I express my deepest gratitude to all relatives, friends and others who in one way or another shared their support.

LIST OF ABBREVIATION AND ACRONYMS

BCWC	Body-Centric Wireless Communication
RF	Radio Frequency
COPD	Chronic Obstructive Pulmonary Disease
UART	Universal Asynchronous Receiver/Transmitter
STM	ST Microelectronics
PCB	Printed Circuit Board
ZP	Zimmer and Peacock
SMA	Subminiature Version a Connector
ISM	Industrial, Scientific, and medical radio band
MRI	Magnetic Resonance Imaging
SAR	Specific Absorption Rate
BSN	Body Sensor Network
BAN	Body Area Network
IEEE	Institute of Electrical and Electronics Engineers
MIC	Microwave Integrated Circuits
PC	Personal Computer
USB	Universal Serial Bus
FR4	Flame Resistant n.4
VSWR	Voltage Standing Wave Ratio
R _{in}	Antenna Resistance
X _{in}	Antenna Reactance
RL	Return Loss
MSPA	Micro Strip Patch Antenna
f _H	Highest frequency
f _L	Lowest frequency

List of Figures

Figure 1.2.1 Body sensor network system [3]	11
Figure 1.3.1 Design circuit [6]	13
Figure 2.3.1 Complete MICS communication network.....	18
Figure 2.4.1 Transmitting Antenna Circuit [32]	19
Figure 2.4.2 Return loss in dB and corresponding VSWR values [33]	21
Figure 3.1.1 Micro strip patch antenna design.....	24
Figure 3.2.1 Design dimensions.....	26
Figure 3.2.2 FR4 substrate	28
Figure 3.3.1 The first design of the patch antenna.....	29
Figure 3.3.2 S-parameter in dB at 2.45 GHz	30
Figure 3.3.3 Far field for $\phi = 90$ for Polar	30
Figure 3.3.4 E-field at 2.45 GHz	31
Figure 3.3.5 S-parameter at 2.452 GHz	32
Figure 3.3.6 Zref at 2.45 GHz	33
Figure 3.3.7 S-parameter at 2.4501 GHz	33
Figure 3.3.8 S-parameter at 2.449 GHz	34
Figure 3.3.9 Optimal patch antenna design at 2.45 GHz	35
Figure 3.3.10 S-parameter at 2.447 GHz	35
Figure 3.3.11 Reference impedance vs frequency	36
Figure 3.3.12 VSWR vs frequency.....	36
Figure 3.3.13 Radiation pattern for $\phi = 90$ in Polar	37
Figure 3.3.14 Radiation pattern for $\phi = 0$ in Polar	37
Figure 3.3.15 Radiation pattern in Cartesian for $\phi = 90$ degrees.....	38
Figure 3.3.16 Radiation pattern in Cartesian for $\phi = 0$ degrees.....	38
Figure 3.3.17 3D radiation pattern.....	39
Figure 3.3.18 E-field at 2.45 GHz	39
Figure 3.3.19 H-field at 2.45 GHz.....	40
Figure 3.4.1 Patch antenna(top layer).....	41
Figure 3.4.2 Ground plane(bottom layer).....	41
Figure 3.4.3 Antenna layout(top).....	42
Figure 3.4.4 Photograph of fabricated antenna	42
Figure 3.5.1 Antenna design.....	43
Figure 3.5.2 S-parameter in dB at 403 MHz	44
Figure 3.5.3 Zref at 403.2 MHz.....	44
Figure 3.5.4 VSWR against frequency	45
Figure 3.5.5 Radiation pattern for $\phi = 0$ in Polar	45
Figure 3.5.6 Radiation pattern for $\phi = 90$ in Polar	46
Figure 3.5.7 Radiation pattern for $\phi = 0$ in Cartesian.....	46
Figure 3.5.8 Radiation pattern for $\phi = 90$ in Cartesian.....	47
Figure 3.5.9 3D polar of micro strip patch antenna.....	47

Figure 4.1.1 Fabricated antenna with SMA connector	48
Figure 4.1.2 Both sides connected with	48
Figure 4.2.1 S-parameter measured	49
Figure 4.2.2 Photo of the measurement of the antenna matching	50
Figure 4.2.3 Sensor board	51
Figure 4.2.4 Photo of sensor	51
Figure 4.2.5 Prototype circuit	53
Figure 4.2.6 Demonstration of the data sent.....	54
Figure 4.2.7 Data read at the receiver	55
Figure 4.2.8 For loop.....	56
Figure 4.2.9 Structure used in sending the data.....	57

Tables

Table 1	Patch antenna parameters.....	43
----------------	--------------------------------------	-----------

Table of Contents

1	Introduction	10
1.1	General Introduction	10
1.2	Work Focus	11
1.3	Personal Contribution.....	12
2	Antenna for Biomedical Applications: Background and Literature Review	14
2.1	Antennas in Lossy Media.....	15
2.2	Design of the Single Antenna	16
2.3	Frequency of Design.....	17
2.4	Antenna Fundamentals.....	18
2.4.1	RADIATION PATTERN	18
2.4.2	INPUT IMPEDANCE	18
2.4.3	VOLTAGE STANDING WAVE RATIO.....	19
2.4.4	RETURN LOSS	20
2.4.5	ANTENNA EFFICIENCY	22
2.4.6	ANTENNA GAIN	22
2.4.7	BANDWIDTH.....	22
3	Methodology and Design of the Antenna	23
3.1	Micro Strip Patch Antenna	23
3.2	Antenna Design Specifications	24
3.2.1	Determination of the MSPA Shape Dimensions	24
3.2.2	Calculating the Substrate Dimensions Ls and Ws	27
3.2.3	Selection of Resonant Frequency.....	27
3.2.4	Specifications of the Substrate.....	27
3.2.5	Feeding Selection.....	28
3.2.6	Selection of the Feed Point Location	28
3.3	Simulation Process at 2.45 GHz	29
3.4	Ki Cad Antenna Design	40
3.5	Simulation Process at 403 MHz (400 – 406 MHz)	43
4	Experimental Results and Discussion	48
4.1	SMA soldering	48

4.2	Fabricated antenna measurements	49
4.3	Sensor used.....	51
4.4	Data transmission	52
5	Conclusion and future work	58

1 Introduction

1.1 General Introduction

A key area of research in the development of healthcare and biomedical technology is body-centric wireless communication (BCWC). A new era of biomedical devices has emerged as a result of improved healthcare quality, continuous sensor miniaturization, advancements in wearable electronics, embedded software, digital signal processing, and biomedical technologies. This has increased the possibility of ongoing disease monitoring, diagnosis, and/or treatment. The radio channel that the communication occurs across is the primary distinction between BCWC and regular wireless systems, particularly implantable devices.

The human body is a harsh place for radio waves to propagate. The radio channel features and implanted antenna performance are all significantly impacted by this environment's extreme loss. In this framework, the main goal of this thesis is to study the importance of using implanted human body antennas for biomedical applications.

This work focuses on designing a micro strip patch antenna connected to a biomedical sensor which sends the sensed data using Bluetooth at 2.45 GHz frequency. This thesis is organized as follows: Chapter 1 describes the introduction about antennas in biomedical applications, chapter 2 presents the state of art (literature review), chapter 3 represents the methodology for RF and antenna design for biomedical applications, chapter 4 presents simulation results and discussion, and finally chapter 5 illustrates the conclusion and future work.

1.2 Work Focus

Research on implantable devices is gaining traction for a variety of uses in both people and animals. Applications include tracking dependent humans or lost pets, tracking blood pressure and temperature, and wirelessly sending diagnostic data from a pacemaker or other implanted electronic equipment to an external RF receiver for human care and safety [1]. Numerous individuals' lives could be improved by tiny, implanted biomedical devices. Patients who have had an antenna implanted in their bodies visit the hospital on a regular basis for checks so that both their health and the implant's condition can be confirmed. While the patient waits in the waiting room, data collected by the implanted antenna can be wirelessly sent to the receiver with the use of RF technology [2]. Figure 1 shows an example of implanted device for health monitoring [3].

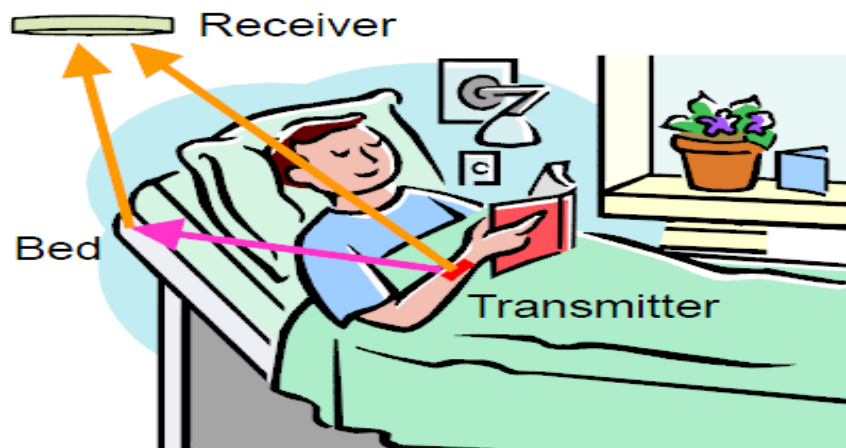


Figure 1.2.1 Body sensor network system [3]

The primary uses of implanted devices are either diagnostic data collection and transmission or therapeutic applications, like the treatment of hyperthyroidism. The impact of continuous

monitoring for many pathogens, including the heart rate, blood oxygen consumption levels in patients with chronic obstructive pulmonary disease (COPD), blood sugar levels in diabetic patients, blood pressure, and patients' daily activities, is demonstrated by medical and biomedical scientists [4, 5]. The quality of healthcare diagnosis, treatment, and medical research are all being improved through implantable devices. Applications like these have encouraged research on implanted antennas, a crucial component of implantable wireless devices. Due to the numerous obstacles that must be overcome, especially for antennas that are surrounded by very lossy media, these fields of study are still in their infancy and offer a great deal of potential. Due to electromagnetic absorption in body tissues, the human body lowers the emitting element's radiation effectiveness [4]. The extremely lossy medium modifies the radiation gain and has an impact on the characteristics and performance of antennas. As a result, among the most difficult aspects of implanted devices is still the performance of implanted antennas. This field of research encourages us to concentrate on enhancing implanted performance of the antenna using various performance improvement methods.

1.3 Personal Contribution

By having the ability to monitor the health of the patients continually and remotely while also collecting relevant signals from the body, implanted antennas play a crucial part in medicine and healthcare. However, there is still a long way to go before we have the optimum high performance transmitting antennas.

This thesis focuses on designing and analyzing a micro strip patch antenna connected with an SMA connector on a PCB (with FR4 substrate). This PCB will be connected to another board which is STM32 Nucleo which includes the embedded system including SMA connector. Both boards are

connected with a male to male SMA connector. The ZP sensor board will be connected to the STM. Our goal is to transmit data that will be asked for from the biosensor using this STM. The data will be taken from the sensor through UART protocol and transmitted to the receiver by Bluetooth at 2,45 GHz (ISM band). And then, the data received is to be displayed using a cellphone. The goal is to design a more efficient micro strip patch antenna for 2.45 GHz applications (including WIFI, Bluetooth), fabricating and designing the hardware design.

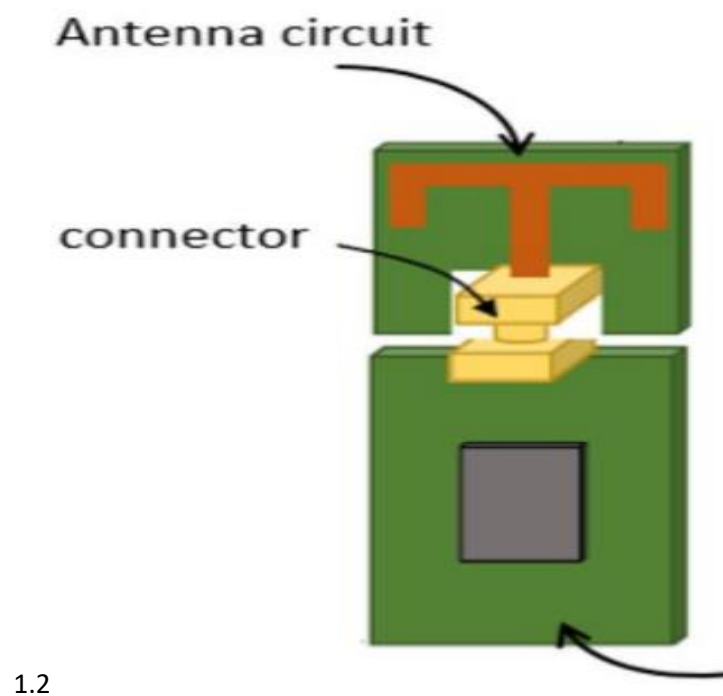


Figure 1.3.1 Design circuit [6]

2 Antenna for Biomedical Applications: Background and Literature Review

Medical implants that can communicate wirelessly with an outer (of a body) device are known as implantable devices. Since the turn of the last century, radio frequency has been created from electromagnetic for use in therapeutic diagnostics. The field of biomedical applications is becoming increasingly interested in implanted devices. Generally, radio frequency and inductive networks are utilized for biomedical interaction [7]. Implanted biomedical devices are now widely accepted and used in a variety of medical applications, including intracranial pressure monitoring, radiometer/heating, dental antenna for remote health care applications, continuous real-time pressure measurements, sugar level checking, pacemaker connection, insulin push out, endoscopy, and blood pressure readings. In reality, these devices play a crucial role in the diagnosis, care and prevention of disease in humans. Applications for implanted antennas in diagnostics range widely, including magnetic resonance imaging (MRI) and may require an implanted antenna [8]. The quality of life is much improved when patients may participate in regular everyday activities rather than staying in the hospital or at home; thanks to long-term monitoring of their activities under physiologically normal conditions. Moreover, by continuously monitoring certain illness changes, for instance, implantable devices improve healthcare quality by lowering the likelihood of particular diseases' complications [9, 10]. Therefore, the monitoring of patients throughout their regular daily activities is the most significant benefit. Thus, ongoing and remote monitoring would take the place of the conventional clinical monitoring [11]. The quality of life will be significantly improved, diagnostic accuracy will be increased and healthcare expenses will be decreased [12].

2.1 Antennas in Lossy Media

This section contains information about the performance of implantable antennas, the difficulties in designing them, and the effects of some key elements that are crucial to their effectiveness. These factors include the antenna's strength, bandwidth, specific absorption rate (SAR) and size.

Using wireless communication in the human body encompasses a broad range of applications that are now known as Body Sensor Network (BSN), Body Area Network (BAN) or Body-Centric Wireless Communication (BCWC) and is formally defined by IEEE 802.15 as "a communication standard optimized for low power devices and operation on, in, or around the human body (but not limited to humans) to serve a variety of applications including medical, consumer electronics, personal entertainment and security" [13].

Implanted devices have numerous applications in the context of biotelemetry, i.e. biomedical wireless communication, to transfer physiological information such as blood pressure, cardiac beat, hyperthermia, and so on [14]. The location of the implanted devices is determined by the telemetry application. Antennas, for example, are located in the brain for a wireless RF powered brain machine interface application [15], or in some applications, as reported in [16], they can be implanted under the skin.

One of the most difficult aspects of designing implantable devices is that some of them must be placed deep within the body. These difficulties are less severe for antennas implanted beneath the skin. The position of the implanted antenna and the electrical properties of the insulating layer are shown to affect RF power reception in [16], and the properties of the tissues surrounding the implanted antenna can influence the electrical characteristics of the antennas. The main focus of

this thesis is on the implanted antennas on bone structures. These specific antennas are used to track the healing of broken bones.

A waveguide antenna with circular polarization that provides bio-medical wireless telecommunication is designed in [17] to monitor the healing of the broken bone.

To investigate the functionality and fabrication challenges of loop antennas, first model the interesting part of the human body and study the effect of relative permittivity of bio tissues on the implanted antenna resonance, as done in [18] and [19].

2.2 Design of the Single Antenna

Antennas should be small enough to be physically implantable inside the human body. The electromagnetic performance of antennas, on the other hand, decreases as their size decreases.

To reduce the size of the antennas, various techniques have been used. Designing the implantable antenna in a folded or spiral shape is one technique proposed in [20] to reduce its size. Another technique for reducing the size of an antenna is to design it at a higher frequency, such as 5.8 GHz [21]. Some studies use a substrate with a high dielectric constant to reduce the size of the antennas, but antennas with a high dielectric constant substrate are susceptible to surface wave excitation, which degrades the antenna's radiation pattern [22, 23]. Implanted antennas can be used to deliver energy for cancer treatment employing hyperthermia techniques [24].

A very small power supply should be installed in the implantable medical device, which is made up of two main circuits: a data telemetry circuit that operates at 402 MHz in a sleep mode and a wake up circuit that receives a wake up signal from an external device, as discussed in [25]. Implantable antennas are intended to operate inside the human body.

2.3 Frequency of Design

The industrial, scientific and medical radio band (433.1-434.8 MHz, 868-868.6 MHz, 902.8-928 MHz, and 2400-2500 MHz) is a group of radio bands or parts of the radio spectrum that are internationally reserved for the use of radio frequency (RF) energy for scientific, medical, and industrial requirements rather than communications. ISM bands are generally open frequency bands that vary depending on region and permit [23]. The optimized design should be at the center of the 2.4 - 2.5 GHz Industrial, Scientific, and Medical (ISM) radio band, i.e., at 2.45 GHz.

The US Federal Communication Commission has oversight over two ISM frequency bands: MICS (402-405 MHz) and (2.4–2.47GHz). The electrical and electromagnetic properties of human tissue [26] have been studied in order to transmit reliable data with high performance, in addition to lower power consumption, as well as technical and medical design factors, ranging from biocompatibility [27, 28], patient safety [28] and miniaturization.

A helical folded dipole and a slot dipole antenna have both been presented as potential dipole antennas for use in medical implant communication applications, specifically for patient monitoring systems. When a loop antenna with a 10 mm diameter is utilized, as opposed to a dipole, the magnetic field is less impacted by body tissue.

Finally, micro strip patch antennas are widely utilized in [29] and [30] due to their low volume, light weight, low profile planar configuration, low manufacturing cost, simplicity of integration with microwave integrated circuits (MICs) and dual and triple frequency operations as shown in figure 2.3.1 [31].

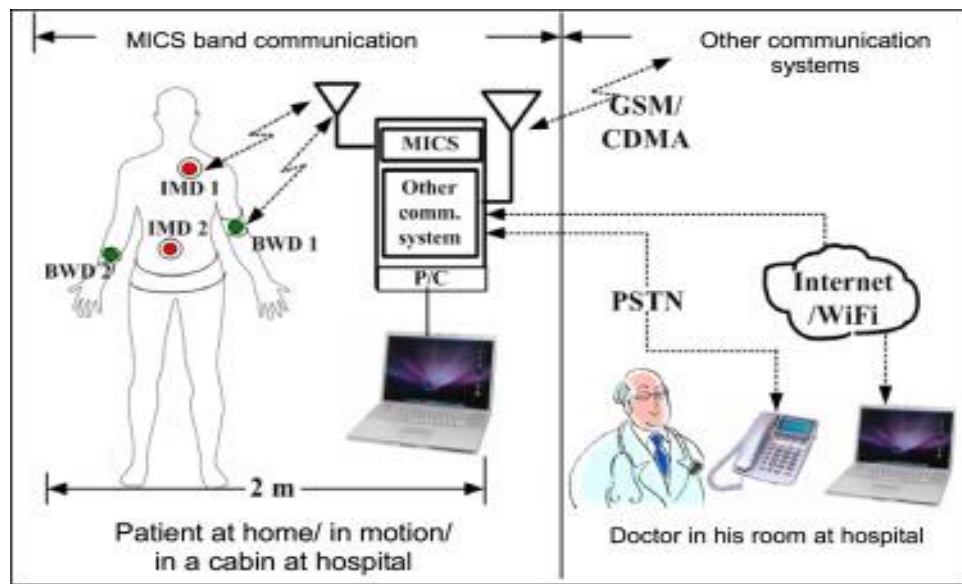


Figure 2.3.1 Complete MICS communication network

2.4 Antenna Fundamentals

2.4.1 RADIATION PATTERN

It is a plot of an antenna's far-field radiation properties with regards to the spatial coordinates identified by the elevation and azimuth angle. This pattern plot is determined by the spatial coordinates. An isotropic antenna radiates identically in all directions.

2.4.2 INPUT IMPEDANCE

Equation 2.1 gives the input impedance:

$$Z_{in} = R_{in} + jX_{in} \quad (2.1)$$

where Z_{in} is the antenna input impedance, R_{in} is the antenna resistance, and X_{in} indicates by the antenna reactance. X_{in} is the imaginary part describing the near-field power stored in the antenna. R_{in} refers to the resistive part of input resistance, which is made of loss resistance and radiation resistance.

2.4.3 VOLTAGE STANDING WAVE RATIO

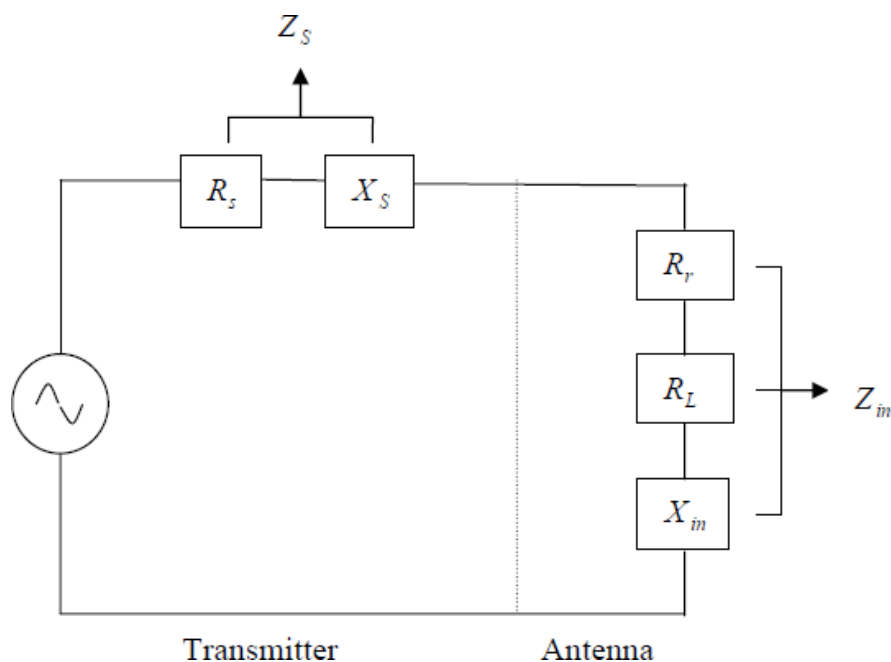


Figure 2.4.1 Transmitting Antenna Circuit [32]

For an antenna to be efficient, it needs the maximum power transfer between the antenna and the transmitter. If the impedance of the antenna matches that of the transmitter, more power will be transmitted.

The voltage standing wave ratio (VSWR) measures how competently RF power is transmitted

from a power source to a load through a transmission line.

The condition is given by equation 2.2;

$$Z_{in} = Z_s^* \quad (2.2)$$

where $Z_{in} = R_{in} + jX_{in}$ and $Z_s^* = R_s + jX_s$

VSWR is given in equation 2.3;

$$VSWR = (1 + \Gamma)/(1 - \Gamma) \quad (2.3)$$

where Γ is the reflection coefficient at the antenna input port. The VSWR is a measurement of the impedance inconsistency between the antenna and the transmitter. When the VSWR is large, we can conclude that it is a high mismatch, but when the VSWR is equal to one, there is a perfect match. VSWR of an efficient antenna should not be more than 2 for the antenna to radiate and transmit in an efficient way.

2.4.4 RETURN LOSS

It is the amount of power lost to the load because it is not reflected back to the input.

The return loss shows how the antenna and transmitter were matched.

It is denoted by and calculated as in reported in equation 2.4 [32]:

$$RL = -20 \log_{10} \Gamma \quad (2.4)$$

When the reflection coefficient is equal to zero, then we have that RL is equal to infinity. This indicates that there is matching impedance load.

For an antenna to work without problems, VSWR can be equal to 2 since it gives an RL of -9.54 dB.

Return Loss in dB	What It Means	VSWR Number
0 dB	100% reflection, no power into the antenna, all reflected back	Infinite
1 dB	80% reflection, 20% power into the antenna	17
2 dB	63% reflection, 37% power into the antenna	9
3 dB	50% reflection, 50% power into the antenna	6
5 dB	32% reflection, 68% power into the antenna	3.5
6 dB	25% reflection, 75% power into the antenna	3
8 dB	16% reflection, 84% power into the antenna	2.3
10 dB	10 dB (10% reflection, 90% power into the antenna)	2
15 dB	15 dB (3% reflection, 97% power into the antenna)	1.4
20 dB	20 dB (1% reflection, 99% power into the antenna)	1.2

Figure 2.4.2 Return loss in dB and corresponding VSWR values [33]

2.4.5 ANTENNA EFFICIENCY

It is the amount which considers the losses that happen at the antenna's terminals and its structure. In other words, it is equal to the radiated power of the antenna with respect to the input power accepted by the antenna.

2.4.6 ANTENNA GAIN

Antenna gain is proportional to antenna directivity. The ability of an antenna to strongly radiate energy in one preferred direction relative to other directions is referred to as directivity. All antennas emit more energy in some directions than others.

2.4.7 BANDWIDTH

The bandwidth of a patch antenna is very small or a narrowband. Many factors can lead to increasing it such as increasing the height of the substrate used (FR4, etc...) with a small permittivity, feeding of probes, making slots, decreasing the length of the patch antenna, or by changing the shape of the antenna used. The micro strip patch antenna working at ISM band has around 100 MHz Bandwidth, but actually it is a bit smaller than this value.

The percentage of the bandwidth for the band we are using is as follows:

$$\% BW = (f_H - f_L)/f_c * 100 \text{ where } f_c = (f_L + f_H)/2$$

Following this equation, and taking f_H 2.5 GHz and f_L 2.4 GHz, we have that the % of the bandwidth is equal to 4.08% of the resonant frequency. This means that the bandwidth is equal to around 100 MHz.

3 Methodology and Design of the Antenna

3.1 Micro Strip Patch Antenna

Microstrip patch antennas have advantages, in comparison with other antennas, since they are tiny, weightless and easy to integrate with other communication devices, which makes them convenient for wireless communication systems.

An antenna is a component of a transmitting and receiving system. This system can also be configured to receive or emit electromagnetic waves. An antenna is a transducer that converts transmission-line signals into electromagnetic field space, which consists of magnetic and electric field patterns moving at right angles to each other in far field. Radiation occurs because of time-varying current when the velocity of charge changes increasingly or decreasingly.

There are different types of microstrip antennas: patch antennas, slot/traveling antennas and printed dipole antennas. Microstrip patch antennas are one of those three types. Choosing an appropriate substrate material is the first step in antenna design.

The most common type of printed antenna is the microstrip antenna. Microstrip patch antennas are the most frequently used type of microstrip antenna due to its several shapes, where the patch in an (MSPA) is typically made of a conducting material such as copper or gold. The microstrip patch antenna can be any shape, but the most common are rectangular, circular, triangular and elliptical. Typically, the radiating patch and feed lines are photoetched on the dielectric substrate.

Advantages of MSPA:

- Low profile, simple and cheap in manufacturing using modern printed circuit technology; mechanically robust when mounted on a rigid surface,

- Can adapt to both planar and non-planar surfaces,
- Can be designed for any type of geometry.

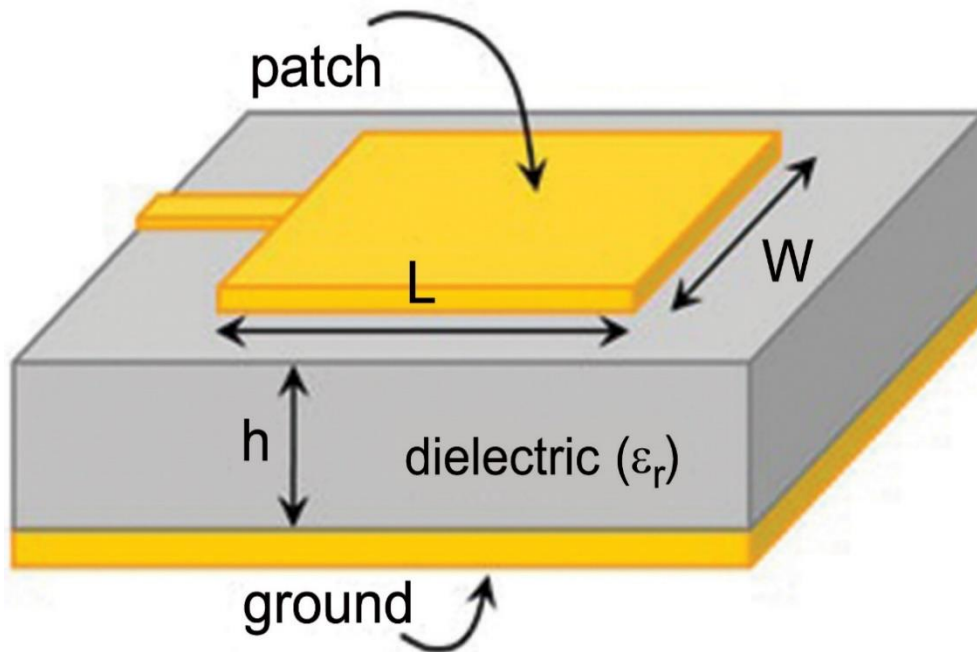


Figure 3.1.1 Micro strip patch antenna design

3.2 Antenna Design Specifications

Taking into account the simulated results on CST suite software, we can introduce initially the shape of the microstrip patch antenna according to the equations.

3.2.1 Determination of the MSPA Shape Dimensions

Step 1: Calculation of the Width of the patch (W) [34]

$$W = \frac{C}{2f_r \sqrt{\frac{\epsilon_r + 1}{2}}}$$

3.1

where f_r is the resonating frequency used, C is the speed of light, ϵ_r is the permittivity of the substrate.

Step 2: Calculation of the Effective Dielectric Constant [34].

$$\epsilon_{\text{eff}} = \frac{\epsilon_r + 1}{2} + \frac{\epsilon_r - 1}{2} \left[\sqrt{\frac{1}{1 + 12 \frac{h}{W}}} \right] \quad \text{for } \frac{W}{h} \geq 1$$

3.2

where h is the thickness of the substrate.

Step 3: Calculation of the Effective length [34]

$$L_{\text{eff}} = \frac{C}{2 f_r \sqrt{\epsilon_{\text{eff}}}}$$

3.3

Step 4: Calculation of the length extension ΔL [34]

$$\Delta L = (0.412 \times h) \left[\frac{(\epsilon_{\text{eff}} + 0.3) \left(\frac{W}{h} + 0.264 \right)}{(\epsilon_{\text{eff}} - 0.258) \left(\frac{W}{h} + 0.8 \right)} \right]$$

3.4

Step 5: Calculation of actual length of the patch [34]

$$L = L_{\text{eff}} - 2\Delta L$$

3.5

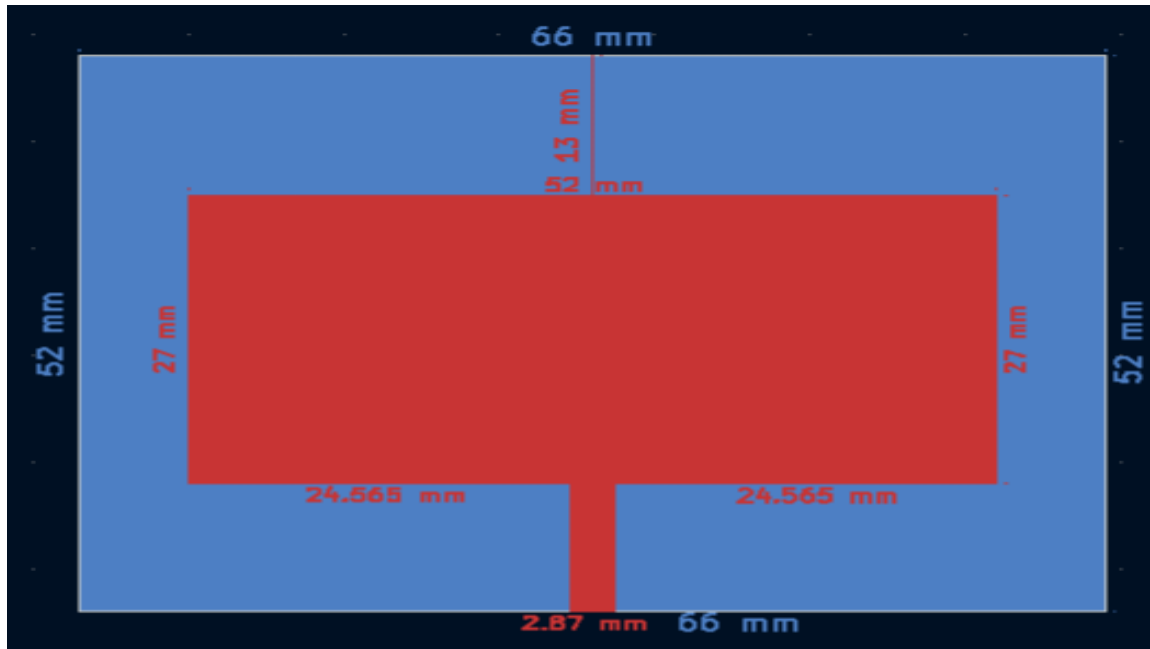


Figure 3.2.1 Design dimensions

Figure 3.2.1 shows the parameters dimensions and the difference between L and ΔL ($L = 27$ mm and ΔL is the difference between the top of the patch antenna and the top of the substrate in this view which equals 13 mm).

3.2.2 Calculating the Substrate Dimensions L_s and W_s

The dimensions of our ground are six times the height of the substrate in addition to the dimensions of the patch antenna.

In this design, the dimensions of the ground plane and the substrate taken are the same.

Equation 3.6 [32] refers to the length of the ground plane and 3.7 is the width.

$$L_s = 6h + L_p \quad 3.6$$

$$W_s = 6h + W_p \quad 3.7$$

3.2.3 Selection of Resonant Frequency

In our study, the frequency used is 2,45 GHz. This frequency is used in ISM band as mentioned above, but I also designed a patch antenna around 400-405 MHz on CST Suite.

3.2.4 Specifications of the Substrate

FR4 glass epoxy is widely used since it is suitable for working under a low and high pressure because of its excellent strength with respect to weight ratios. It has a tangent loss of 0.2 and a dielectric constant equals to 4.5. They can also withstand a variety of temperatures, making them suitable for etching printed circuits. The FR4 substrate is cheap in price and easy to buy from any manufacturer over the Internet. The dimensions for some substrates are altered. The thickness (height) of the substrate is taken as 1.6 mm. The frequency of the work is 2.45 GHz.

The dielectric constant values of other substrates is different.



Figure 3.2.2 FR4 substrate

3.2.5 Feeding Selection

The designed printed antenna with the transmission line are connected to an SMA connector. This connector will be also connected to another SMA on the other side using a male-male SMA connector.

3.2.6 Selection of the Feed Point Location

The impedance where the feed should be will be of 50 Ohm at the frequency required which is 2.45 GHz. Simulations were done to have the exact place of this feed in order to have a good matching. This position will have the minimum return loss in the graph S11 vs Frequency.

3.3 Simulation Process at 2.45 GHz

The values of the desired antenna are taken according to the previous equations mentioned.

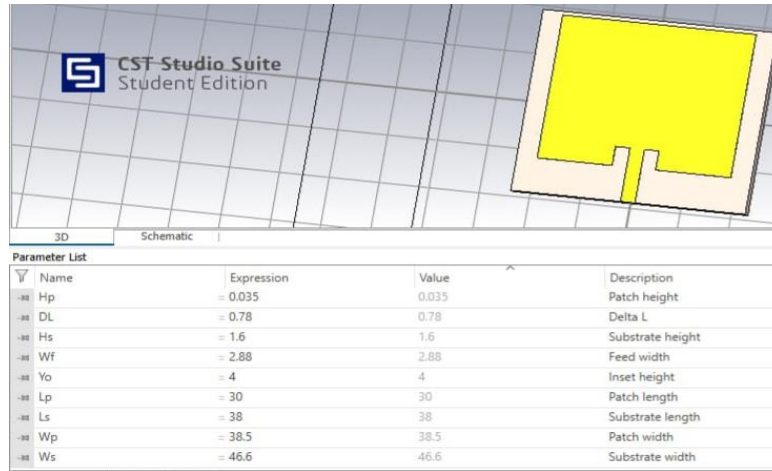


Figure 3.3.1 The first design of the patch antenna

According to this design, the following result shows:

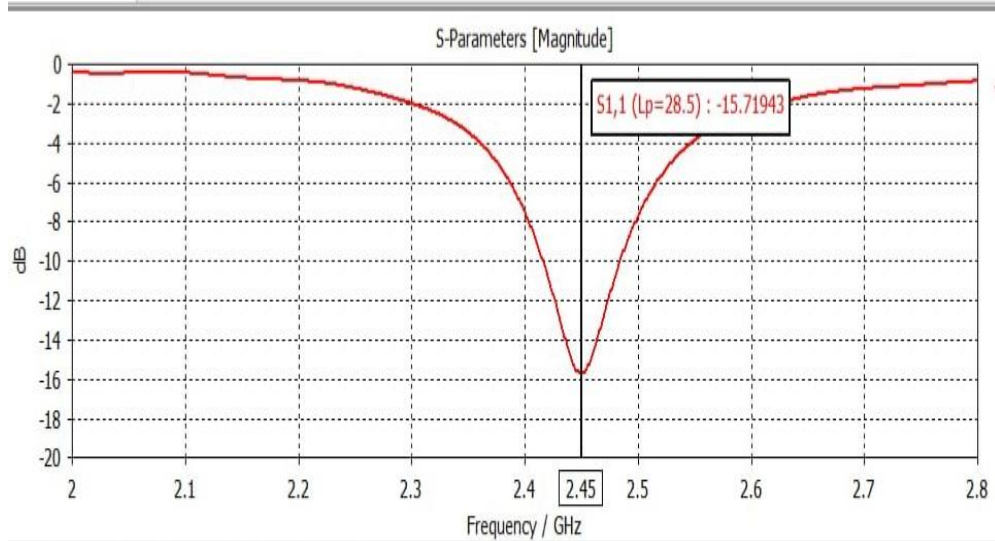


Figure 3.3.2 S-parameter in dB at 2.45 GHz

This graph shows the S11 results of the first design done.

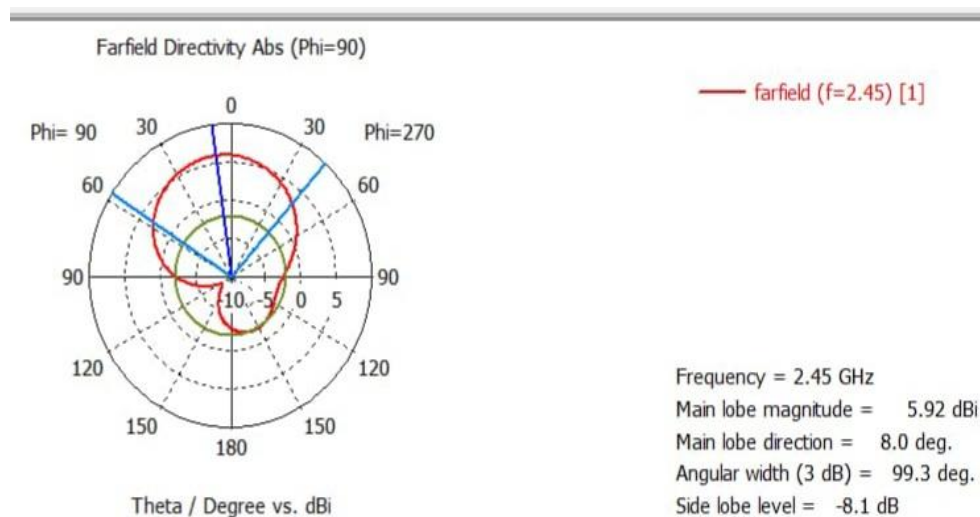


Figure 3.3.3 Far field for phi = 90 for Polar

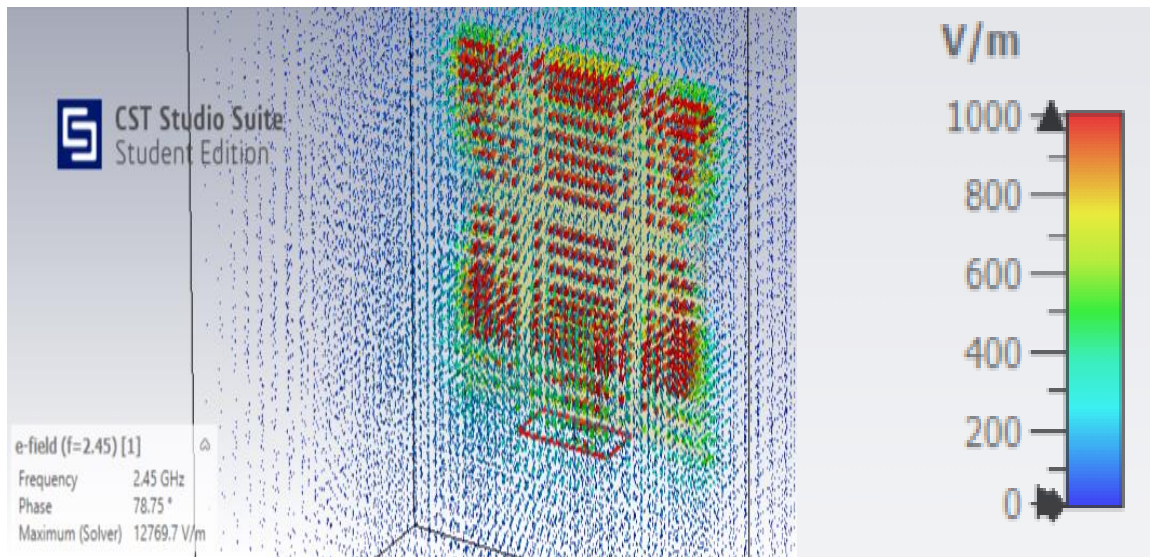


Figure 3.3.4 E-field at 2.45 GHz

Following these results, we have a bandwidth less than 100 MHz which is not acceptable.

We tried to improve our bandwidth by doing a parametric sweep for our parameters that can be changeable.

Now, we changed the value of DL to 6 mm and Ls to 42 mm. S11 is better, but we still have a bandwidth less than 100 MHz.

We are still working on sweeping till reaching the best simulation we want.

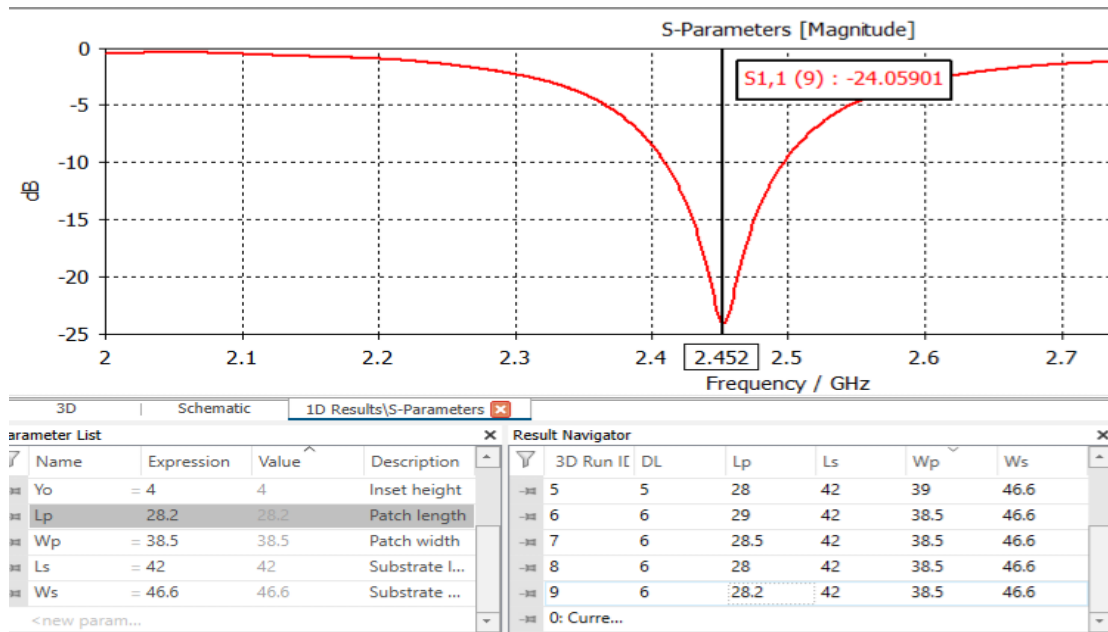


Figure 3.3.5 S-parameter at 2.452 GHz

Decreasing the width of the transmission line to 2.48 mm, Lp equals to 28.35 mm, and Wp is 38.5 leads to increasing in the input impedance and also a variation in S11 with respect to the values in figure 3.3.5. Now the impedance is equal to 55.859 ohms at the resonant frequency. This result is not good for matching.

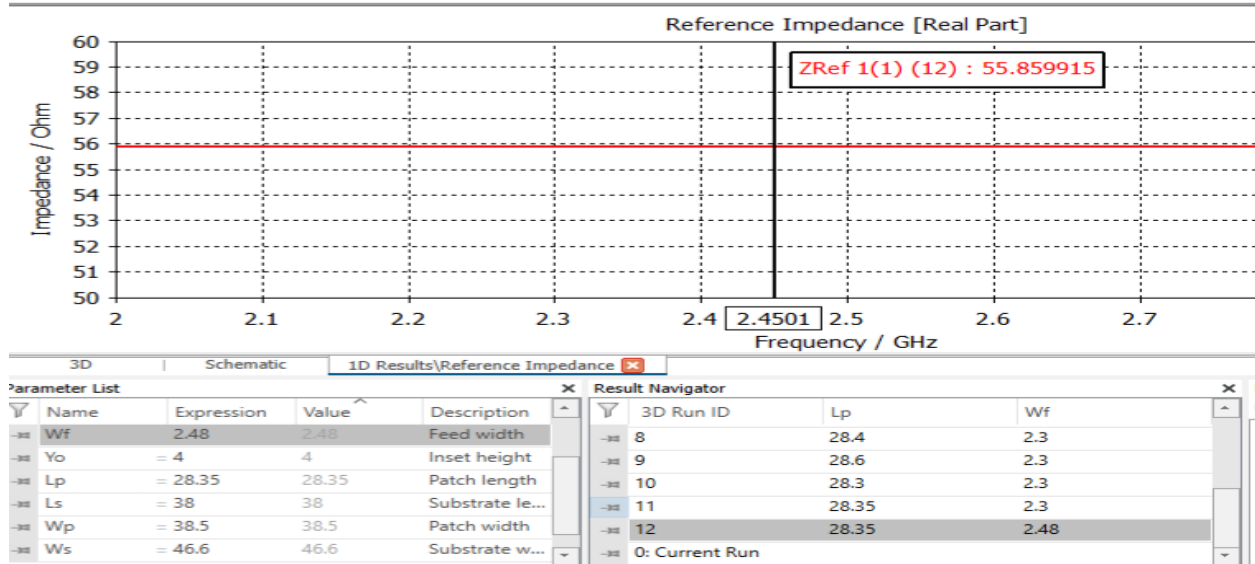


Figure 3.3.6 Zref at 2.45 GHz

Here, Zref is equal to 55.85 Ohm and this means that there is no optimal matching.

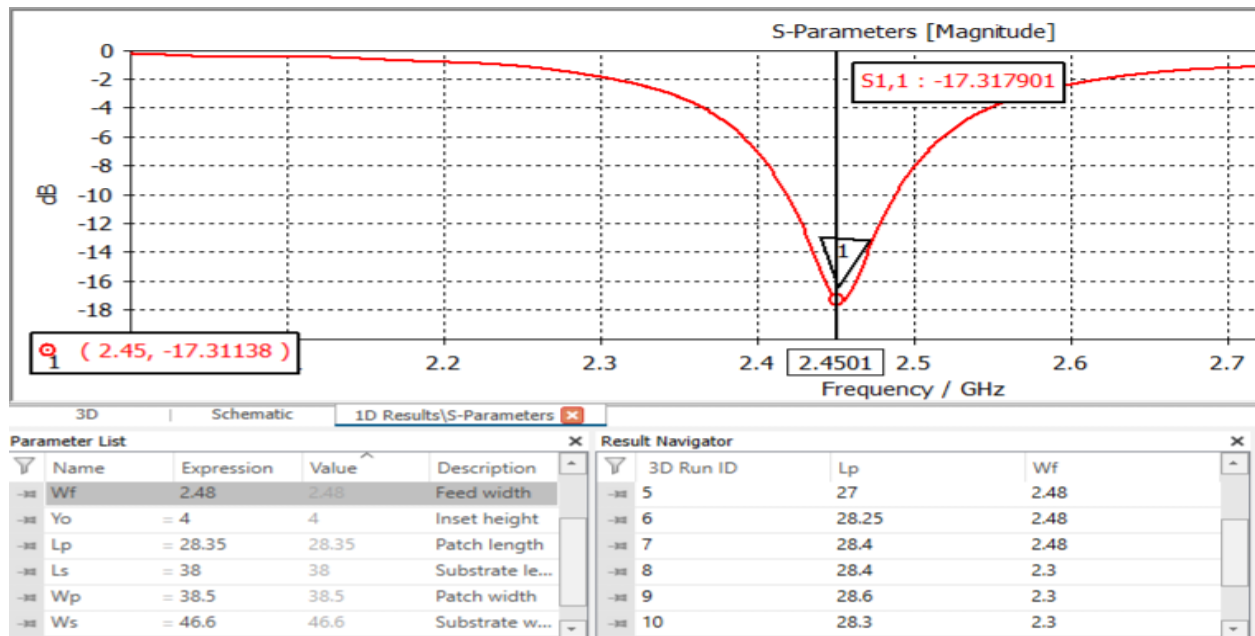


Figure 3.3.7 S-parameter at 2.4501 GHz

We should solve this problem by returning the value of the feedline width as it was. Also, we have to play with other parameters to have the best design.

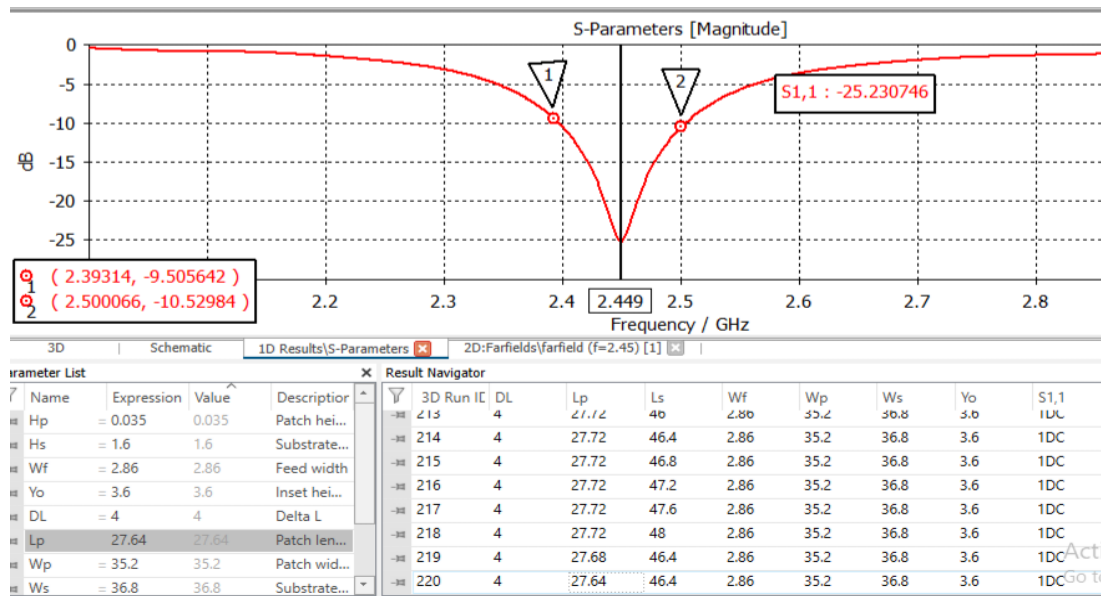


Figure 3.3.8 S-parameter at 2.449 GHz

The change in parameters' values happened, but we have a new problem which is the edges of the patch are very close to the dielectric constant. As we see in 3.3.8, the width of the patch equals 35.2 mm while that of the substrate is 36.8 mm, knowing that we have a good value of S11 at the resonant frequency. This is not the best solution for us since very close edges may lead to a shift during the fabrication process. (The distance is less than 2 cm).

The optimal solution is to enlarge the dimensions and remove the inset that is placed above the transmission line.

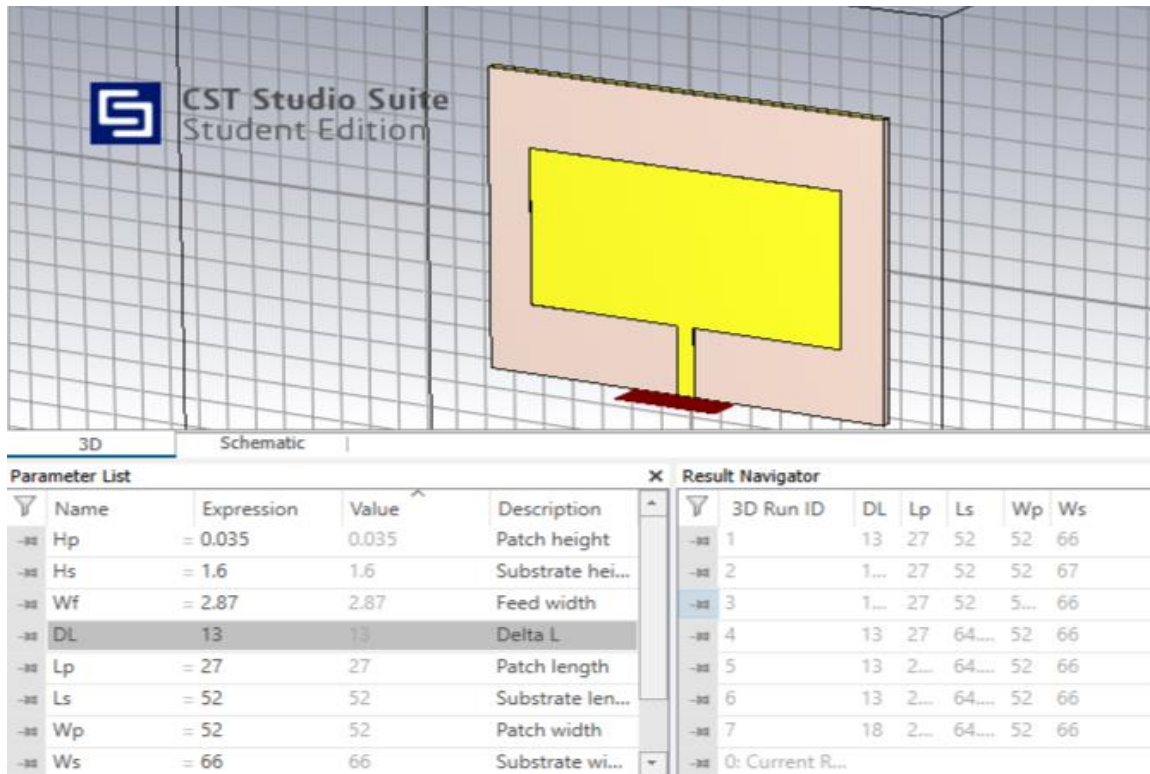


Figure 3.3.9 Optimal patch antenna design at 2.45 GHz

This is the microstrip patch antenna that has the best performance in terms of S11 and characteristics impedance matching.

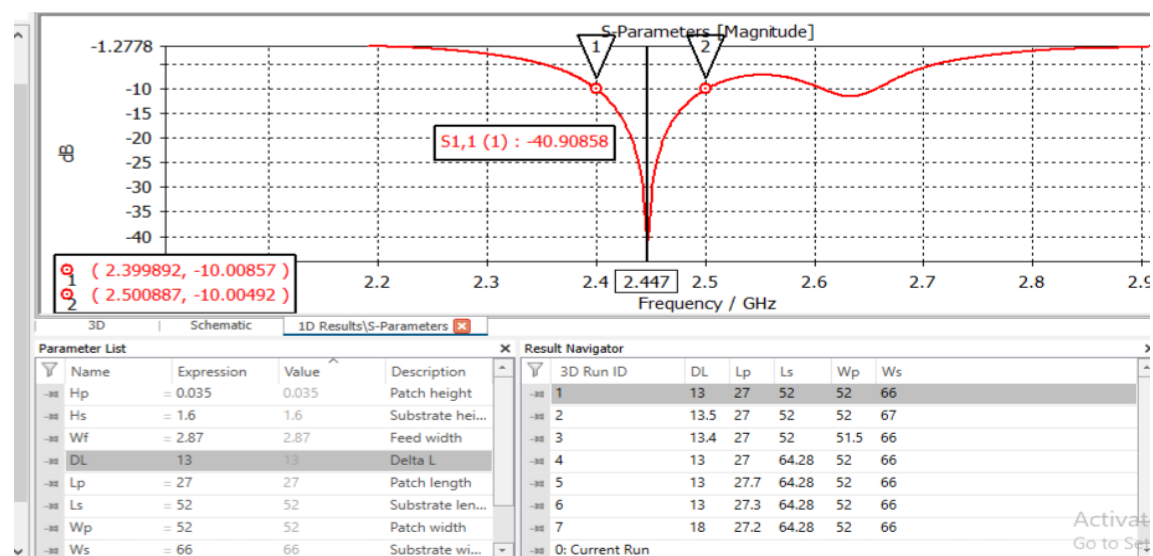


Figure 3.3.10 S-parameter at 2.447 GHz

Here, S11 has the best value in dB calculated; therefore, we can move on depending on these values of our parameters.

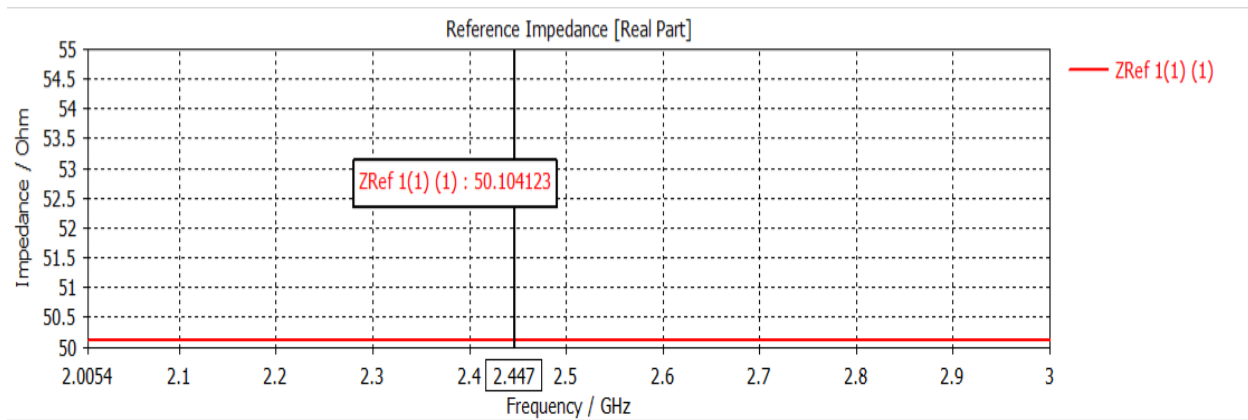


Figure 3.3.11 Reference impedance vs frequency

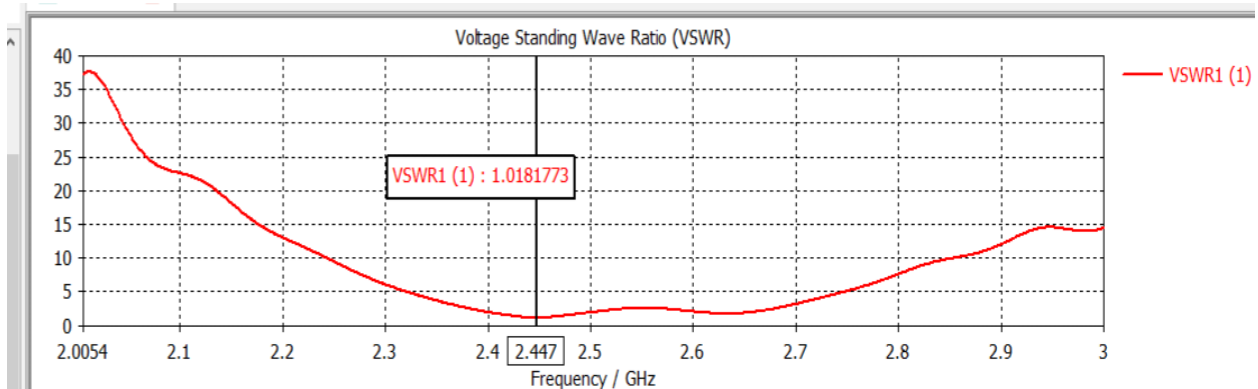


Figure 3.3.12 VSWR vs frequency

This means that the reflection power is too low. (The smaller the VSWR, the better the antenna matching to the feed line and the most power delivered to the antenna).

Other simulations are done to have the radiation pattern graphs in polar and cartesian planes and the gain at the resonant frequency.

Radiation pattern is a graphical representation of an antenna's radiation properties with respect to space. It means that how much the antenna we have, it radiates power out into space.

An antenna should radiate power in all directions. Then, we can say that it is three-dimensional.

The results we obtained describe also the 3D pattern of our antenna.

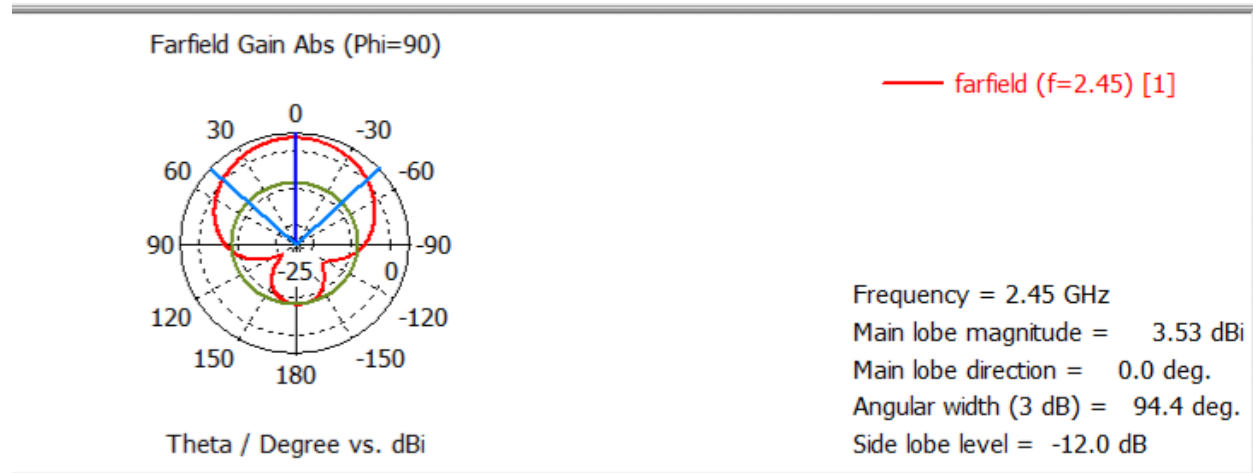


Figure 3.3.13 Radiation pattern for phi = 90 in Polar

Figure 3.3.13 shows the radiation pattern for phi = 90 degrees in polar plane at the resonant frequency 2.45 GHz.



Figure 3.3.14 Radiation pattern for phi = 0 in Polar

This figure shows the same as figure 3.3.13 but for $\phi = 0$ degrees.

As a result, we can also mention the same graphs but in cartesian plane.

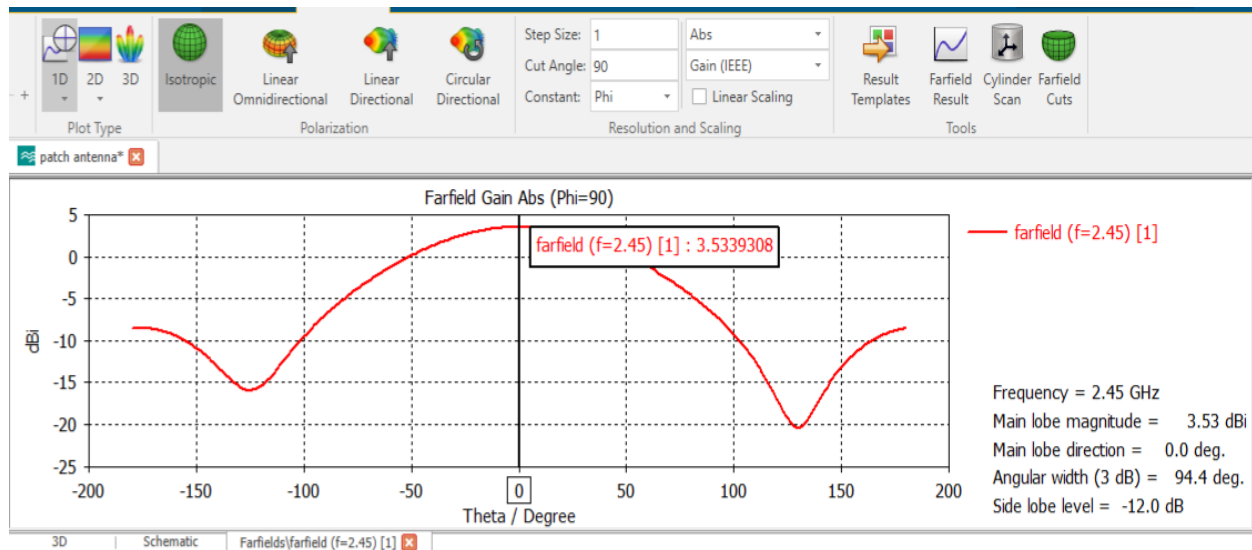


Figure 3.3.15 Radiation pattern in Cartesian for $\phi = 90$ degrees

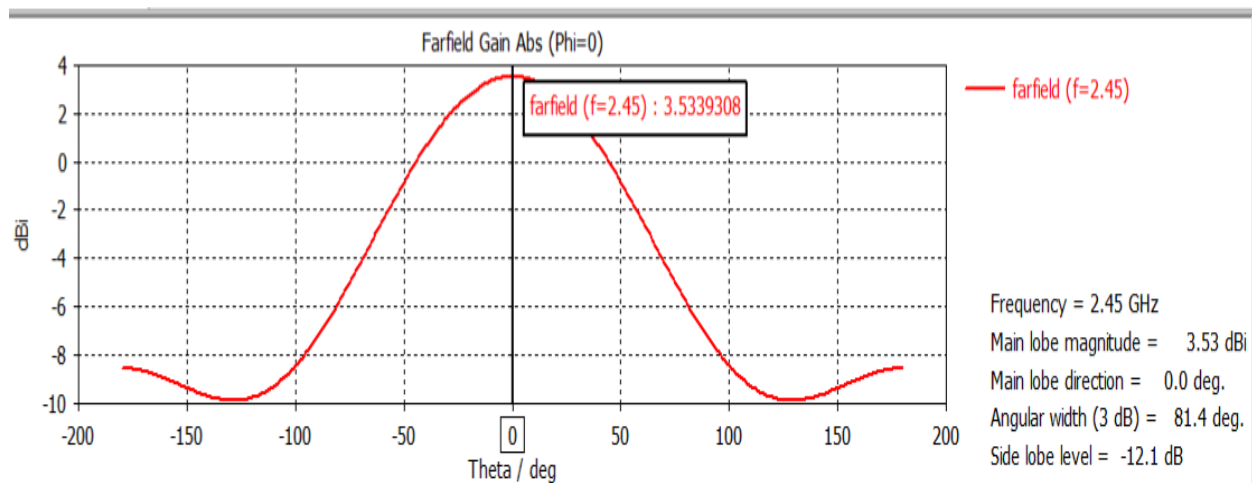


Figure 3.3.16 Radiation pattern in Cartesian for $\phi = 0$ degrees

Now, the gain is equal to 3.534 dBi at 2.45 GHz and the farfield in 3D as follows:

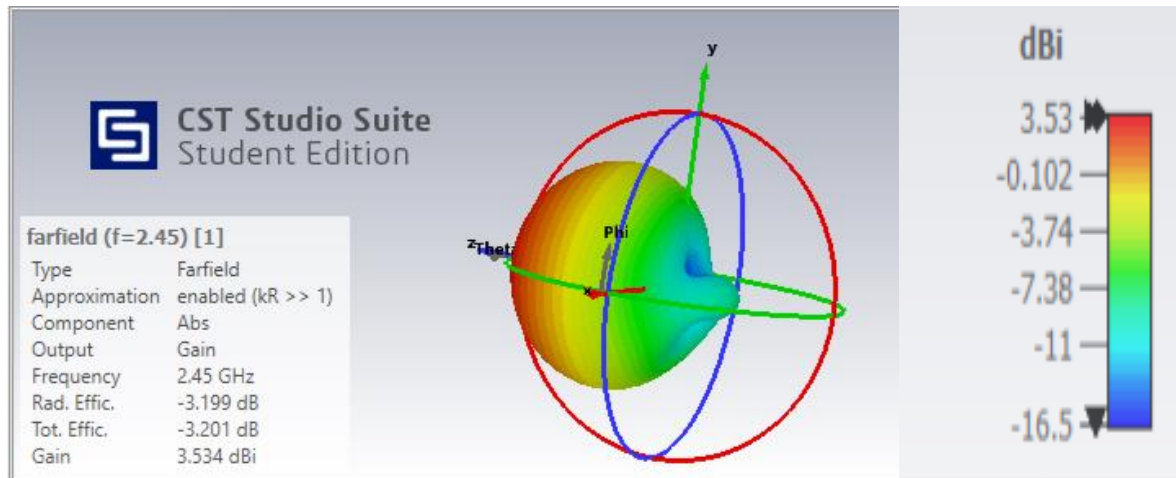


Figure 3.3.17 3D radiation pattern

Also, we can see the E-field and H-field at the resonant frequency 2.45 GHz.

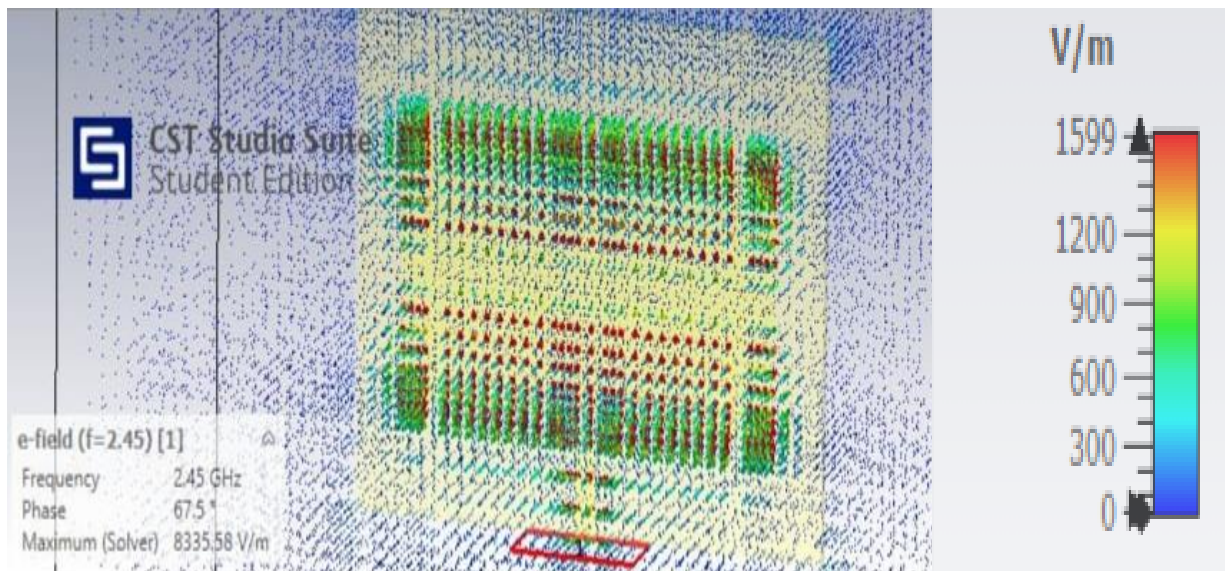


Figure 3.3.18 E-field at 2.45 GHz

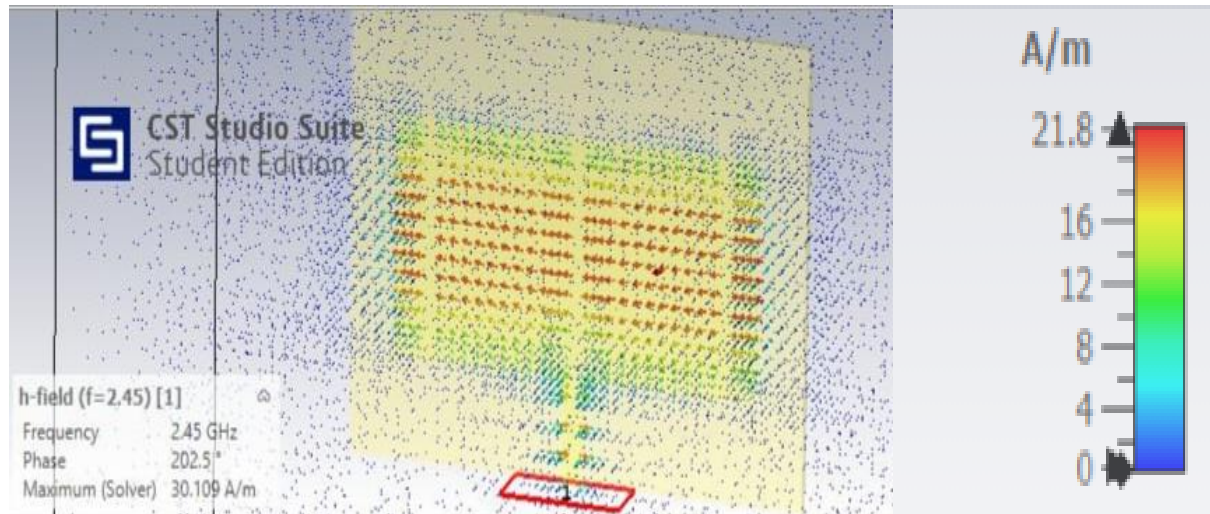


Figure 3.3.19 H-field at 2.45 GHz

Electromagnetic waves are made of electric fields(called E-field) and magnetic fields(H-field). Figure 3.3.18 shows the electric field of the antenna at its resonant frequency which means technically the electric field at a specific point in space is a measurement of how powerful a force would be on a unit point charge. It has a magnitude and direction and measured in V/m. On the other hand, the magnetic field is shown in figure 3.3.19 and is measured in A/m.

3.4 Ki Cad Antenna Design

After simulating our antenna on CST software and having all the simulation results, we want especially a good S11 at the resonant frequency and the best bandwidth we reached at these dimensions designed, it is the time for designing the layout before PCB antenna fabrication.

As we mentioned above, the FR4 substrate has a dielectric constant of 4.5 and the substrate thickness is equal to 1.6 mm. With these specifications, we can move to designing the layout.

Top Layer:

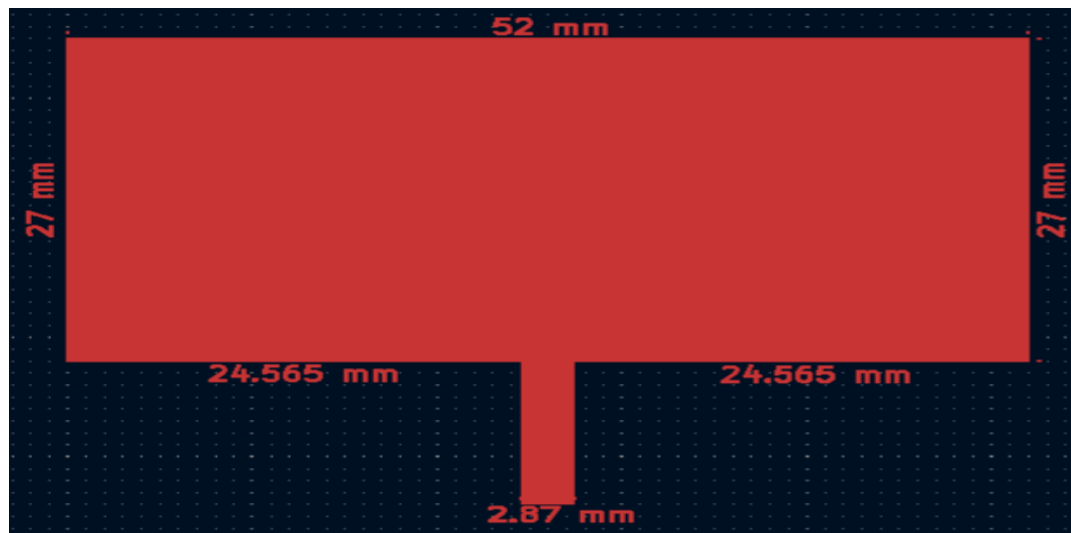


Figure 3.4.1 Patch antenna(top layer)

Bottom Layer:

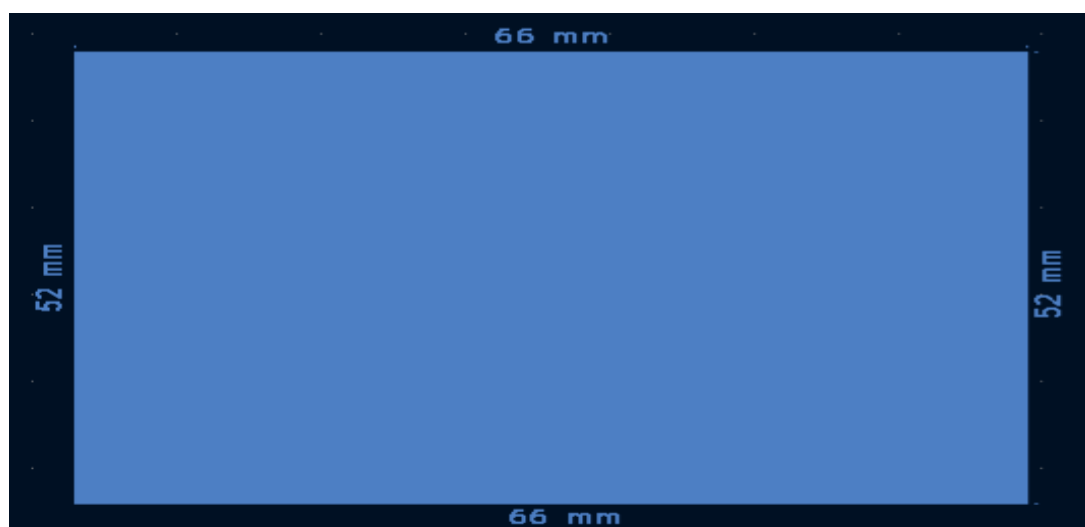


Figure 3.4.2 Ground plane(bottom layer)

The microstrip patch antenna now is ready for fabrication.

As mentioned before, the thickness of the substrate taken is 1.6 mm, dielectric constant is 4.5, loss tan is 0.025, material is FR4, the ground and the antenna are of copper material.

Our goal is to have a good matching between the simulation and the measurement values and graphs.

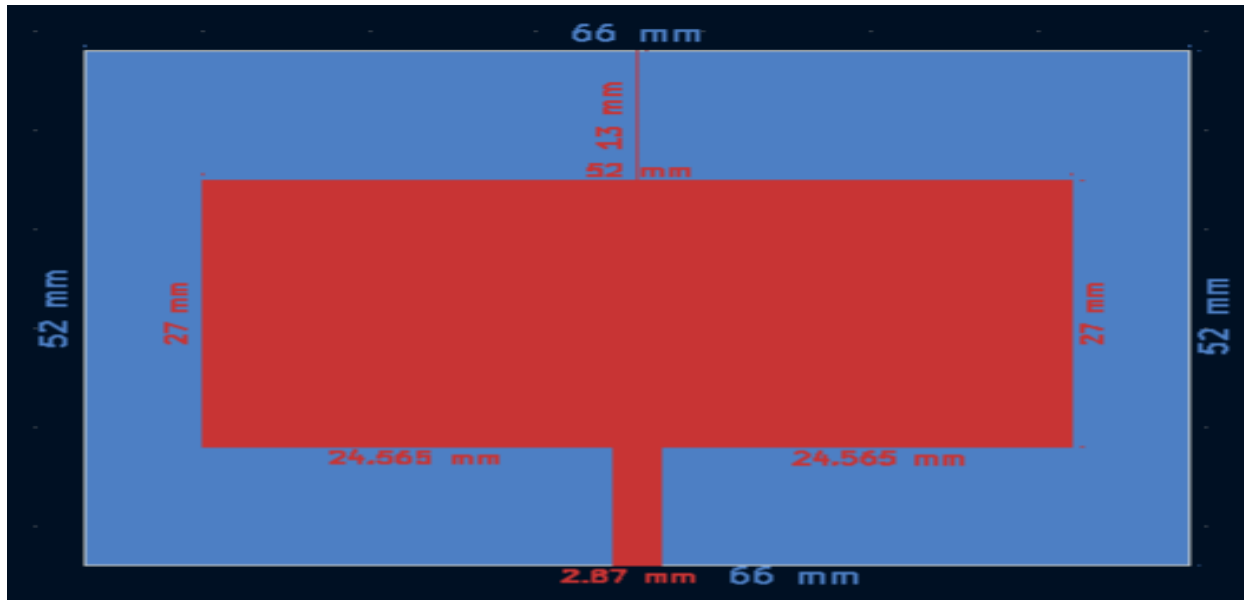


Figure 3.4.3 Antenna layout(top)

After having all the simulations acceptable, it is the time for antenna fabrication.



Figure 3.4.4 Photograph of fabricated antenna

3.5 Simulation Process at 403 MHz (400 – 406 MHz)

The values of this antenna are taken according to the previous equations and has the following values as indicated in Table 1.

Parameter	Antenna dimensions
ϵ_r	4.5
h(substrate thickness)	1.6 mm
W(patch width)	210 mm
L(patch length)	168.2 mm
DL	18 mm
Wg(substrate width)	235 mm
Lg(substrate length)	220 mm
Wf(feedline width)	5 mm
Inset height	4 mm
C(speed of light)	3.0×10^8 m/s
fc(frequency)	403 MHz

Table 1 Patch antenna parameters

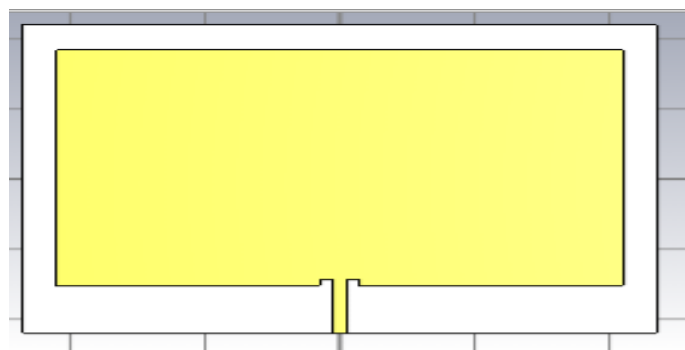


Figure 3.5.1 Antenna design

According to the above design, we have S11 as follows:

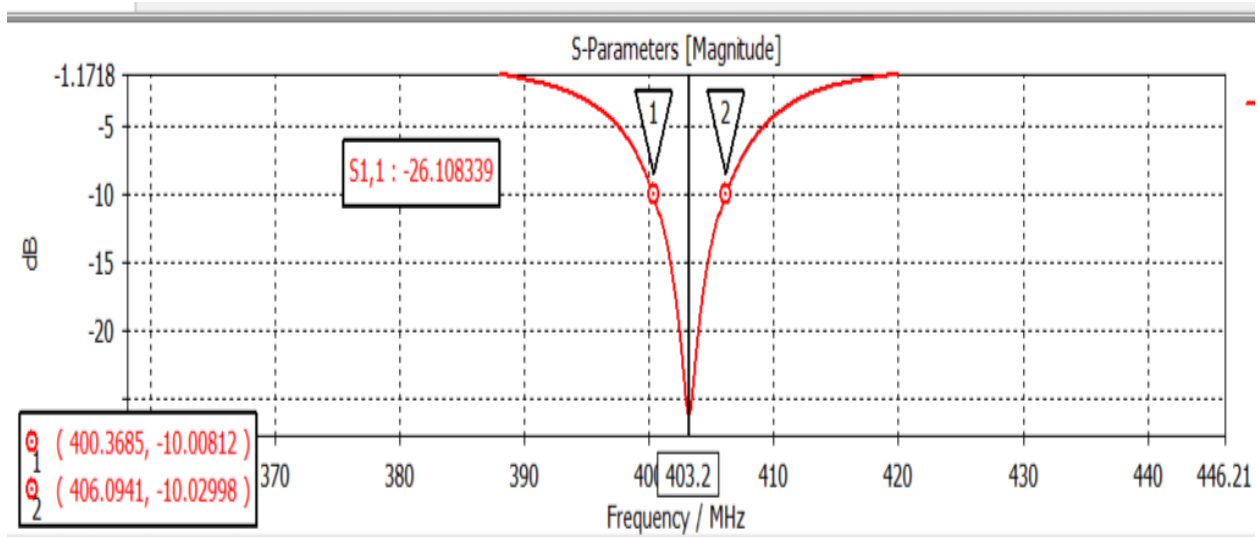


Figure 3.5.2 S-parameter in dB at 403 MHz

Figure 3.5.2 shows the return loss against frequency of the antenna. The resonant frequency for the antenna is 403 MHz and the return loss is – 26 dB. This antenna can transmit or receive a signal efficiently at a frequency between 400.36 and 406.09 MHz.

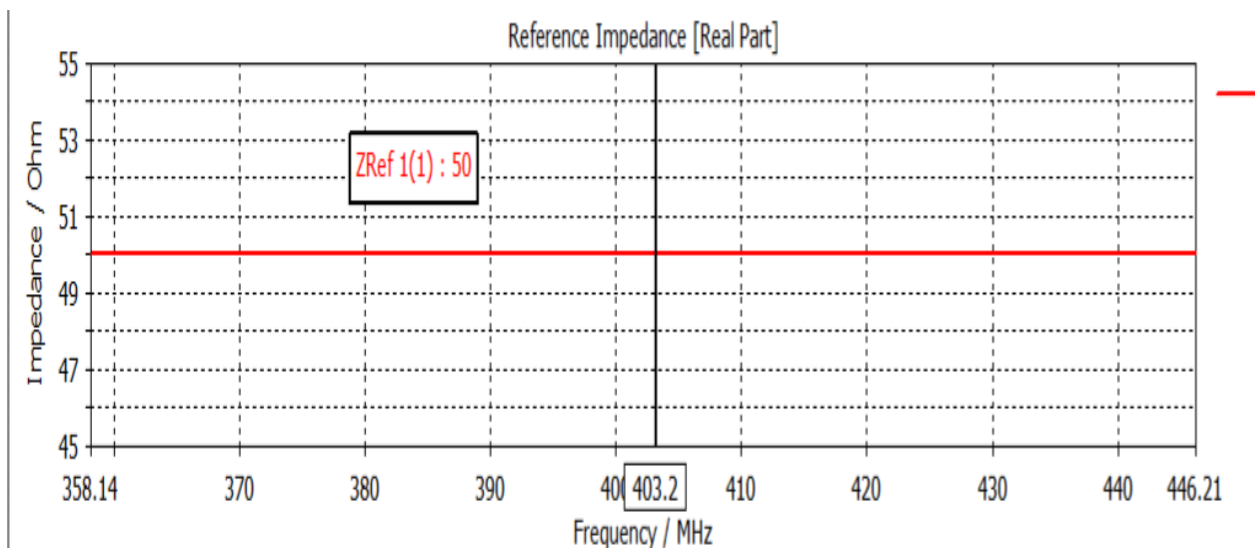


Figure 3.5.3 Zref at 403.2 MHz

Figure 3.5.3 shows the impedance against frequency which is always constant at 50 Ohm.

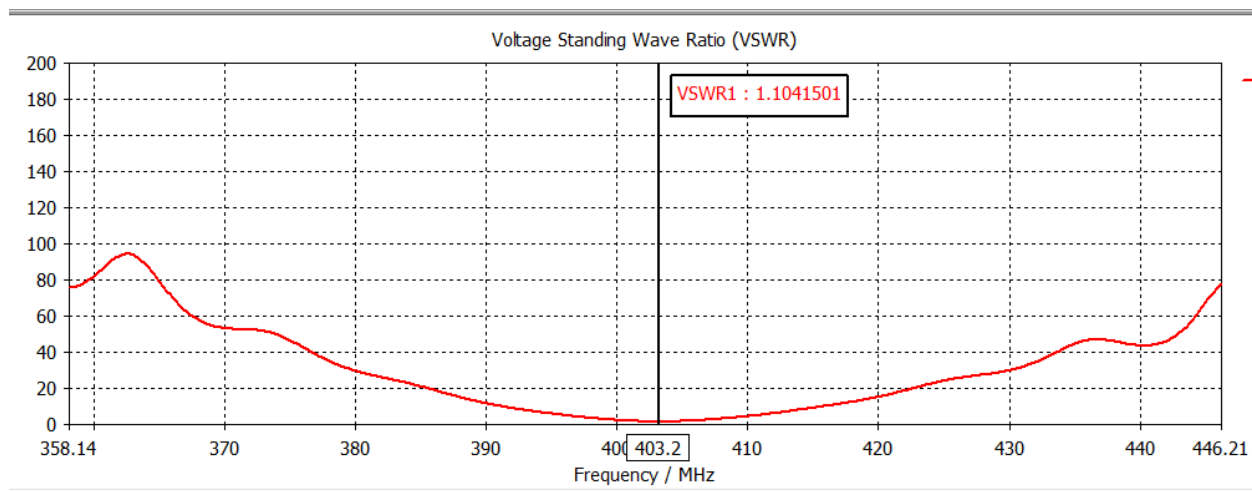


Figure 3.5.4 VSWR against frequency

Figure 3.5.4 shows that the VSWR at the resonant frequency is equal to 1.1. This means that there is a good matching and power reflected is very low.

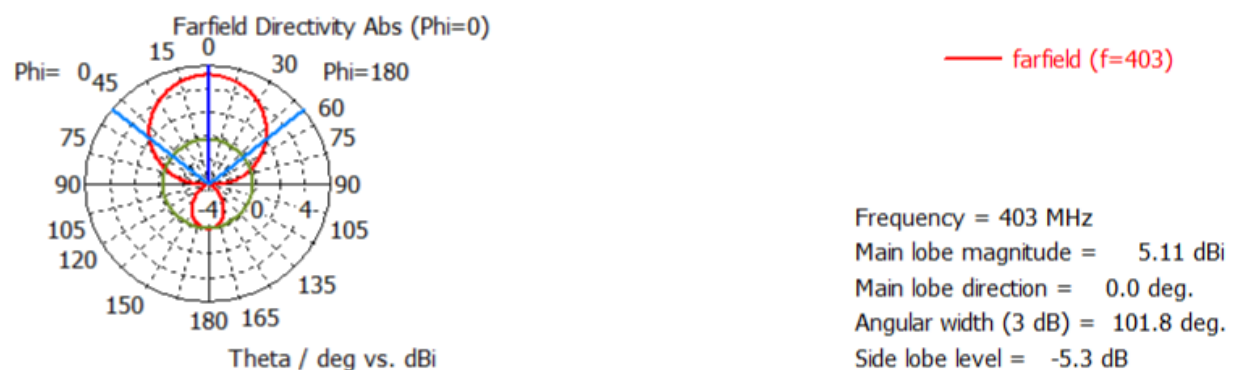


Figure 3.5.1 Radiation pattern for phi = 0 in Polar

Figures 3.5.5 and 3.5.6 state that the antenna can direct the input power into radiations in a given direction more than others. The antenna can transmit or receive a signal in an efficient way in the direction of highest gain. All microstrip antennas radiate highest into one direction at angle of Θ equals 0 degrees that is perpendicular to the antenna.

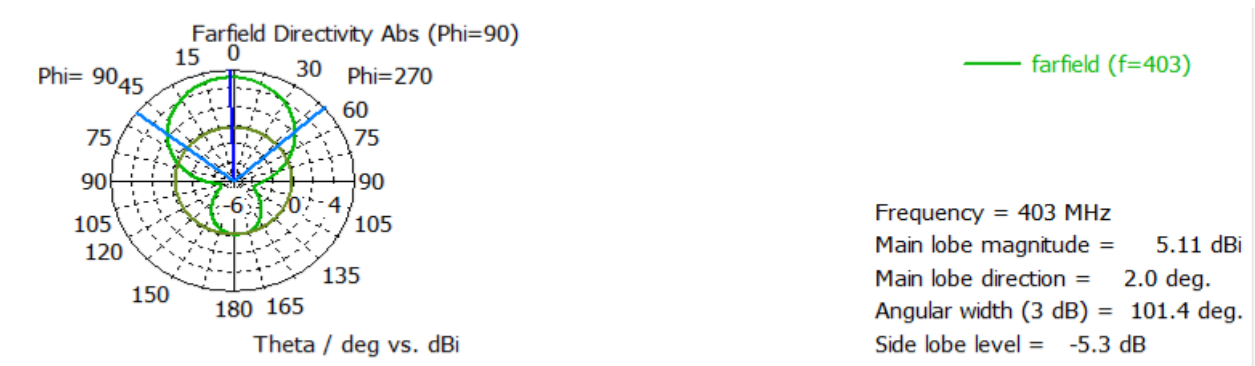


Figure 3.5.1 Radiation pattern for phi = 90 in Polar

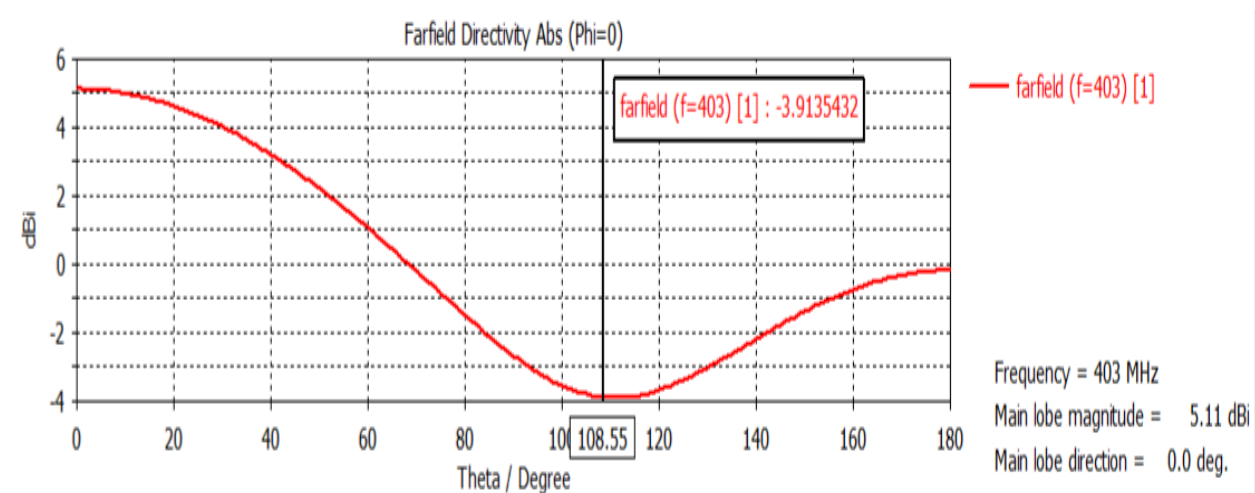


Figure 3.5.1 Radiation pattern for phi = 0 in Cartesian

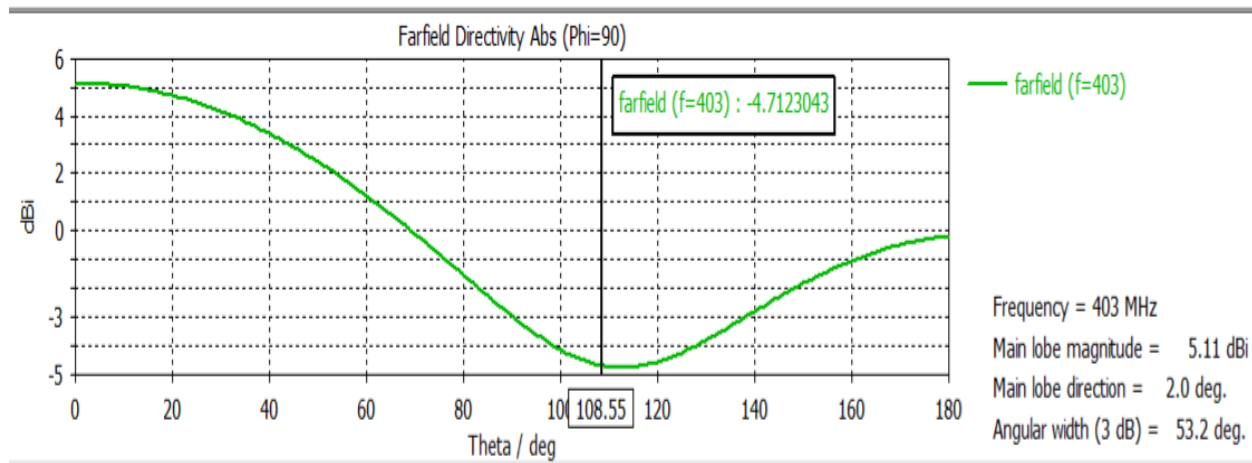


Figure 3.5.1 Radiation pattern for phi = 90 in Cartesian

At frequency equals to 403 MHz, the highest gain of the antenna is 5.11 dB. This means that the antenna can direct the input power into radiations in a direction more than others. The antenna is able to transmit or receive a signal in an efficient way where the direction has the highest gain.

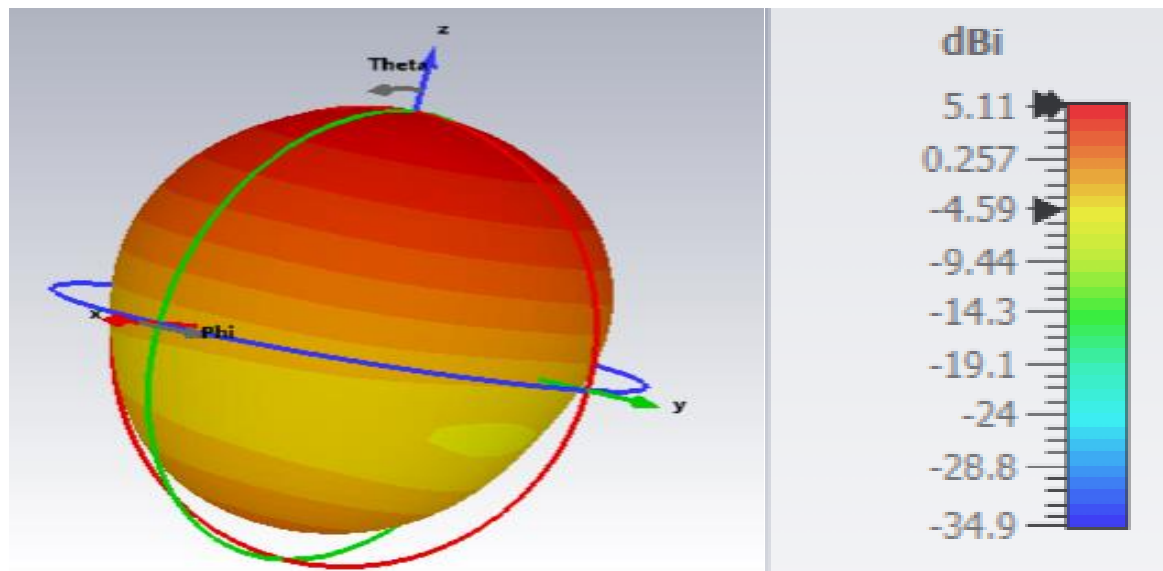


Figure 3.5.2 3D polar of micro strip patch antenna

4 Experimental Results and Discussion

4.1 SMA soldering

First of all, after fabricating the patch antenna we should solder the female SMA connectors for both sides (the antenna and the STM Nucleo) as shown in figures 4.1.1 and 4.1.2, respectively.

After soldering, we put a male-to-male SMA connector that will connect both sides together.



Figure 4.1.1 Fabricated antenna with SMA connector

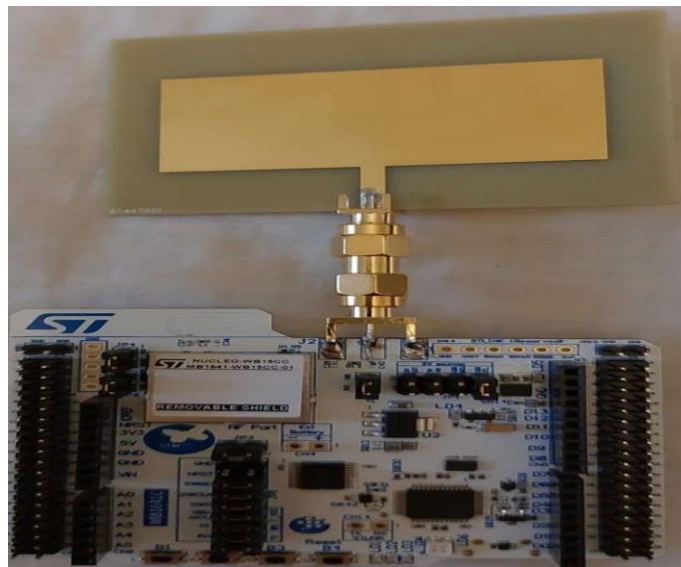


Figure 4.1.2 Both sides connected with male-to-male connector

4.2 Fabricated antenna measurements

The fabricated micro strip patch antenna was connected to the vector network analyzer (VNA). It was able to detect the signal and the return loss curve was displayed on the screen. The curve showed that the micro strip antenna was resonating at 2.484 GHz.

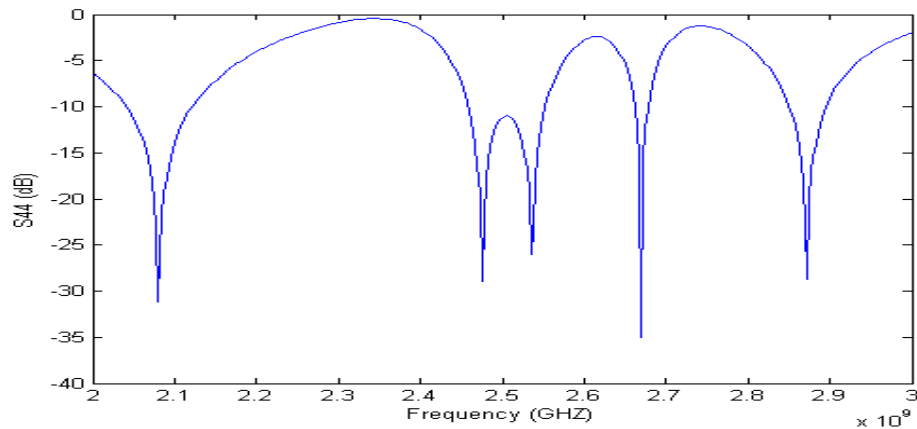


Figure 4.2.1 S-parameter measured

Figure 4.2.1 shows s-parameter of the fabricated antenna. The minimum return loss at the resonating frequency is about -26.86 dB. This means that the reflected power is less than 1 percent, and therefore the antenna is working almost in an optimal way.

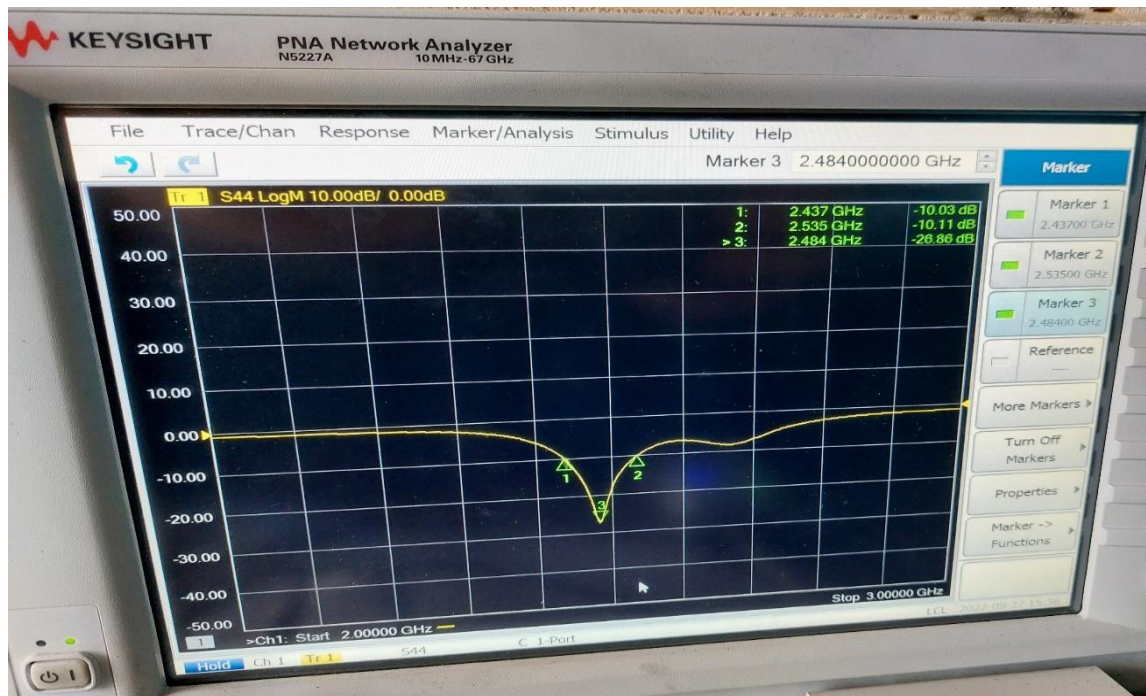


Figure 4.2.1 Photo of the measurement of the antenna matching

The antenna was resonating at 2.484 GHz while the simulated one was resonating at 2.45 GHz. The results are comparable since there was a little deviation in the resonating frequency value. This difference may be a reason of the dielectric constant. It was taken in the simulations and fabrication process 4.5, while it should be a little bit different to have the resonant frequency quite similar to the simulations. From the data sheet, FR4 has a range of values in the dielectric constant (between 3.8 and 4.8).

The frequency in the measurements obtained at -10 dB for both sides were 2.437 GHz and 2.535 GHz as shown in figure 4.2.2 respectively. The bandwidth in the simulations was around 101 MHz, while in the measurements was 98 MHz. Hence, a good agreement between them has been obtained.

4.3 Sensor used

In order to verify and check our system, we have created an embedded system that is composed of a biosensor that can measure several values such as oxygen values in volts, glucose level, pH, or ion concentration. This sensor will be connected to the sensor board which is shown in figure 4.2.3.

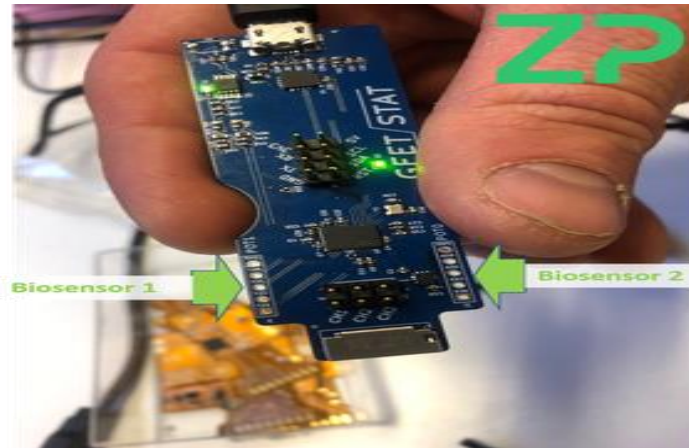


Figure 4.3.1 Sensor board



Figure 4.3.2 Photo of sensor

Figure 4.2.4 shows the photo of the sensor that we will use in the system. It has 3 electrodes, so the working electrode is the black one made of carbon. Zimmer and Peacock can also make customized sensors with the option to target other analytes than those.

4.4 Data transmission

After connecting the antenna and the STM Nucleo board with the connector and having the sensor with the board, we can start testing to transmit and receive the data.

Receiving data will be using an application on a cellphone called BLE tester (A Bluetooth Low Energy test tool). This application can be used to read and write data. BLE mainly uses the CRC algorithm (Cyclic Redundancy Check which is a polynomial-based error detection technique that generates a series of two 8-bit block check characters that represent the entire block of data. These block check characters are embedded in the transmission frame and checked at the receiving end). As widely used check codes, CRC is often used in the data link layer to check whether the network packet is wrong or not. If the test result is wrong, the data will be transmitted another time. Another application was tested but it was not able to receive the data, consequently we cannot use it. The biosensor will read some values (as mentioned above), and these data will be asked for from the microcontroller to transmit it to the receiver via UART protocol (serial data communication) by Bluetooth at our resonating frequency 2.45 GHz. The transmitter and the receiver(the cellphone) are put beside each other(distance less than 1 meter).

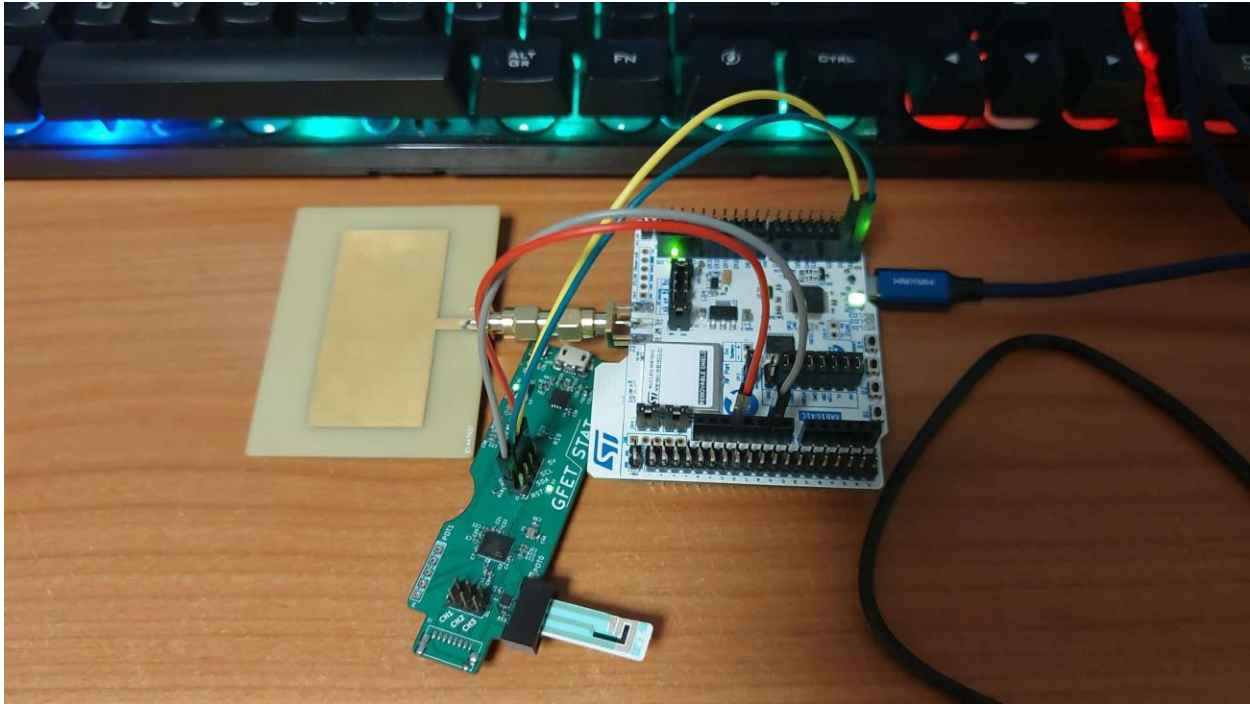


Figure 4.4.1 Prototype circuit

Figure 4.2.5 shows the prototype circuit of the design we have. The antenna is connected to the embedded system(Nucleo) by a connector (as commented before). The ground pin of the sensor is connected to the second pin of CN6 which is the ground. However, the power supply (3V3) of the sensor is connected to 3V3 pin of CN6.

The TX pin of the sensor board is connected D0 pin in CN9 section which is the RX pin, but RX of the sensor is connected to D1 pin in CN9 which is the TX pin.

The Nucleo board and the PC are connected to each other doing the firmware using STM32CubeIDE software and using C language with this software.

Firmware is done by building for release version that will give then a .HEX file. We make a flash of the code on the flash storage using so called ST-linker. Now, we have the code on the microcontroller.

Figure 4.2.6 shows the data read by the sensor and sent to the receiver using UART protocol. The data sent is “index,911 0.241 V”.

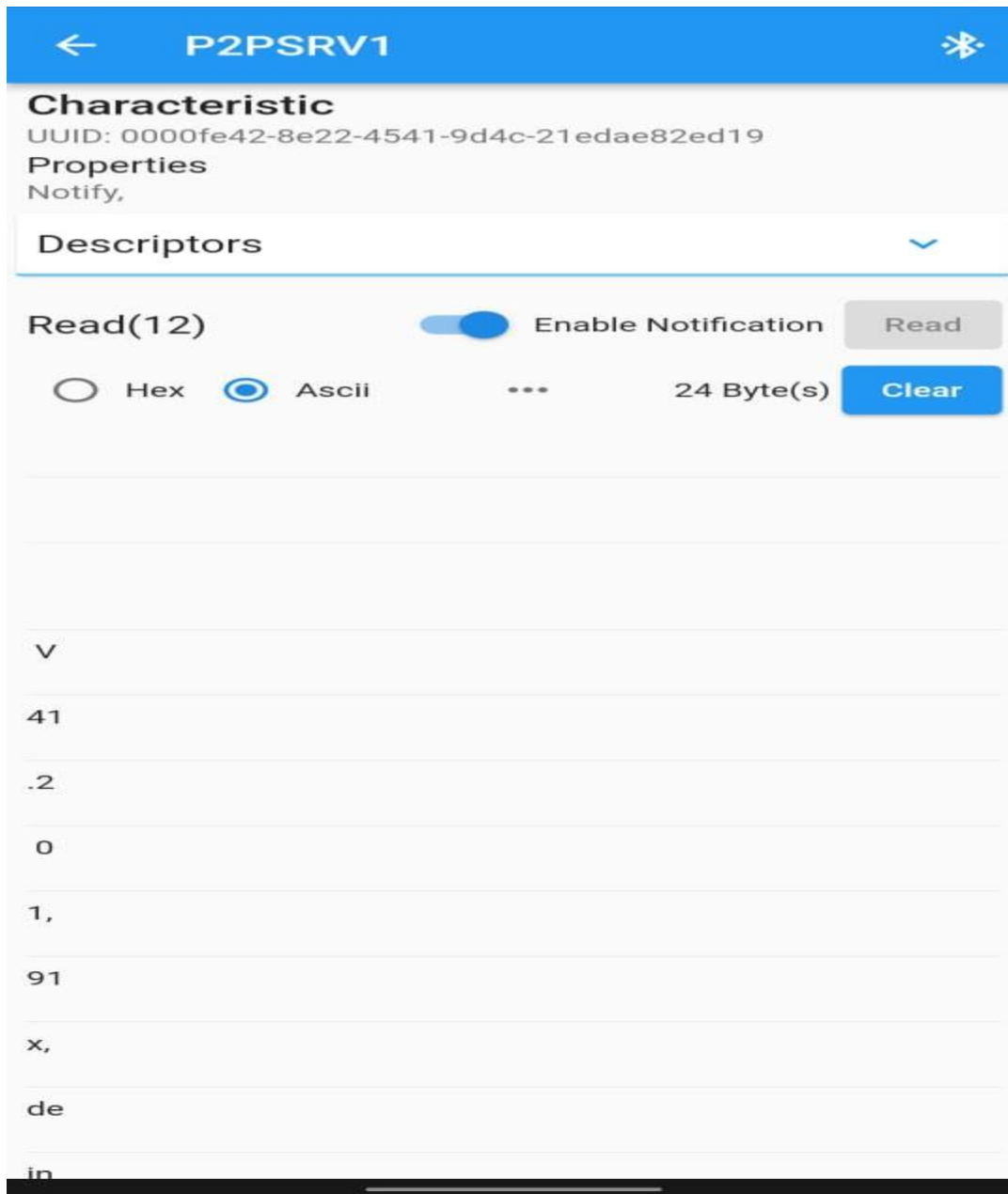


Figure 4.4.3 Data read at the receiver

Figure 4.2.7 shows the data read at the BLE tester application on the cellphone (at the receiver).

These data are totally the same comparing to figure 4.2.6, and means that transmission of the data is working as it should be.

```

HAL_UART_Receive(&huart1, UART1_rxSensorBuffer, 19,5000);

if(isConnected){
    uint8_t *data = &UART1_rxSensorBuffer;
    for (int i=0;i<21;i++){

        P2PS_STM_App_Update_Char(P2P_NOTIFY_CHAR_UUID, data);
        data+=2;
    }
}

```

Figure 4.4.4 For loop

Figure 4.2.8 shows the for loop used to send the data. These data we have, will be sent to the receiver by Bluetooth.

(HAL_UART_Receive) is a method of the HAL library (Hardware Abstracted Layer), that includes the data of the UART used for reading (the configurations), where the place that we will fill in with the data read is the buffer.

If all is working well and connected, the process will start and data will be sent by Bluetooth. The data that will be sent by Bluetooth will be filled in the array uint8_t, and the for loop will start working as sending the data 2 bytes each iteration. Every time we are sending the data will be incremented by 2. For loop has the number of bytes (21) which is the size of the message of the sensor in addition of the terminator (characters for doing termination for a new line) and 5.000 is a timer put to wait for the data from the sensor. If the data is not received after 5 seconds, then data will be sent another time.


```

switch(UUID)
{
    case P2P_NOTIFY_CHAR_UUID:

        result = aci_gatt_update_char_value(aPeerToPeerContext.PeerToPeerSvcHdle,
                                            aPeerToPeerContext.P2PNotifyServerToClientCharHdle,
                                            0, /* charValOffset */
                                            2, /* charValueLen */
                                            (uint8_t *) pPayload);

        break;

    default:
        break;
}

```

Figure 4.4.5 Structure used in sending the data

Figure 4.2.9 shows the structure that will be filled by the data we want to send. It consists of 5 variables; the ones we want to use are the last three. These variables are the offset that is always zero because always it will start from the beginning, the second one is the value of the message we sent which is here 2 bytes, and the last one is the payload that is a pointer on an array of unsigned integer of 8 bits. When this structure is full, there is a service that is pushing on Bluetooth.

5 Conclusion and future work

This thesis presented a design of a PCB antenna at ISM band connected with an embedded system to work for a biomedical application. The goal was to transmit and receive data by Bluetooth. A review of the implantable devices design, challenges and applications were presented.

It was shown that one of the challenges for the antenna performance the dimensions. Several models were simulated to have the more realistic model of the patch antenna. To justify the results, the simulations and the measurements done of the return loss, the bandwidth and and Smith Charts were almost similar. The simulated return loss(S_{11}) at the resonating frequency was around - 41 dB. However, the measured was almost -27 dB. Both values are good since in both cases the reflected power is less than 1 percent which almost the best result. The bandwidth also is not so far, since it is 101 MHz and 98 MHz, respectively.

The data transmission also was succesful since we had the same message received and displayed on the receiver(BLE tester application on cellphone).

The advantage in this project is that SMA connector was used to connect both sides. So, we are looking forward to benefit from the embedded system used in other applications in the future.

References

1. Houzen, T., M. Takahashi, and K. Ito. *Implanted antenna for an artificial cardiac pacemaker system*. in *Progress in Electromagnetics Research Symposium*. 2007.
2. Yuce, M.R., *Implementation of wireless body area networks for healthcare systems*. Sensors and Actuators A: Physical, 2010. **162**(1): p. 116-129.
3. Hall, P., Y. Hao, and K. Ito, *Guest editorial for the special issue on antennas and propagation on body-centric wireless communications*. IEEE Transactions on Antennas and Propagation, 2009. **57**(4): p. 834-836.
4. Marzegalli, M., et al., *Design of the evolution of management strategies of heart failure patients with implantable defibrillators (EVOLVO) study to assess the ability of remote monitoring to treat and triage patients more effectively*. Trials, 2009. **10**(1): p. 1-11.
5. Kupelian, P., et al., *Multi-institutional clinical experience with the calypso system in localization and continuous, real-time monitoring of the prostate gland during external radiotherapy*. Cancer Radiotherapie, 2008. **12**(hors serie1): p. 18-20.
6. Gretsikh, D., et al. *Researching the Possibility of Wireless Energy Transmission for the Power Supply Condition Monitoring System of a Car's Suspension*. in *2020 IEEE Ukrainian Microwave Week (UkrMW)*. 2020. IEEE.
7. Skrivervik, A.K. and F. Merli. *Design strategies for implantable antennas*. in *2011 Loughborough Antennas & Propagation Conference*. 2011. IEEE.
8. Damaj, A.W., H.M. El Misilmani, and S. Abou Chahine. *Implantable antennas for biomedical applications: An overview on alternative antenna design methods and challenges*. in *2018 International Conference on High Performance Computing & Simulation (HPCS)*. 2018. IEEE.
9. Andre, D. and D.L. Wolf, *Recent advances in free-living physical activity monitoring: a review*. Journal of diabetes science and technology, 2007. **1**(5): p. 760-767.
10. Kupelian, P., et al., *Multi-institutional clinical experience with the Calypso System in localization and continuous, real-time monitoring of the prostate gland during external radiotherapy*. International Journal of Radiation Oncology* Biology* Physics, 2007. **67**(4): p. 1088-1098.
11. Garcia-Morchon, O., et al. *Security for pervasive medical sensor networks*. in *2009 6th Annual International Mobile and Ubiquitous Systems: Networking & Services, MobiQuitous*. 2009. IEEE.
12. Zweifel, P., S. Felder, and M. Meiers, *Ageing of population and health care expenditure: a red herring?* Health economics, 1999. **8**(6): p. 485-496.
13. Gutierrez, J.A., et al., *IEEE 802.15. 4: a developing standard for low-power low-cost wireless personal area networks*. IEEE network, 2001. **15**(5): p. 12-19.
14. Zhao, Y., et al. *Simulation of implantable miniaturized antenna for brain machine interface applications*. in *Proc. Adv. CEM Appl. II ACES conf*. 2012.
15. Shokry, M. and A. Allam. *Implanted antenna in brain*. in *2013 Loughborough Antennas & Propagation Conference (LAPC)*. 2013. IEEE.
16. Islam, M.S., et al., *Converting a wireless biotelemetry system to an implantable system through antenna redesign*. IEEE Transactions on Microwave Theory and Techniques, 2014. **62**(9): p. 1890-1897.
17. Zakavi, P., N.C. Karmakar, and I. Griggs, *Wireless orthopedic pin for bone healing and growth: Antenna development*. IEEE transactions on antennas and propagation, 2010. **58**(12): p. 4069-4074.
18. Yazdandoost, K.Y. and R. Miura. *Miniaturized UWB implantable antenna for brain-machine-interface*. in *2015 9th European Conference on Antennas and Propagation (EuCAP)*. 2015. IEEE.

19. Surapan, S., et al. *Design of dual band implantable antenna for biomedical applications*. in 2016 13th International Conference on Electrical Engineering/Electronics, Computer, Telecommunications and Information Technology (ECTI-CON). 2016. IEEE.
20. Abadia, J., et al., *3D-spiral small antenna design and realization for biomedical telemetry in the MICS band*. Radioengineering, 2009. **18**(ARTICLE): p. 359-367.
21. Huang, W. and A.A. Kishk, *Embedded spiral microstrip implantable antenna*. International Journal of Antennas and Propagation, 2011. **2011**.
22. Sánchez-Fernández, C., et al., *Dual-band microstrip patch antenna based on short-circuited ring and spiral resonators for implantable medical devices*. IET microwaves, antennas & propagation, 2010. **4**(8): p. 1048-1055.
23. Merli, F., *Implantable antennas for biomedical applications*. 2011, EPFL.
24. Ibraheem, A. and M. Manteghi, *Performance of an implanted electrically coupled loop antenna inside human body*. Progress In Electromagnetics Research, 2014. **145**: p. 195-202.
25. Chang, C.-L., et al. *Novel triple-band biotelemetry system with miniaturized antenna for implantable sensing applications*. in *SENSORS, 2010 IEEE*. 2010. IEEE.
26. Blanos, P., *Miniaturization of implantable antennas for medical applications*. National Technical University of Athens, School of Electrical & Computer Engineering, Athens, 2013.
27. Kiourti, A. and K.S. Nikita, *A review of implantable patch antennas for biomedical telemetry: Challenges and solutions [wireless corner]*. IEEE Antennas and Propagation Magazine, 2012. **54**(3): p. 210-228.
28. Psathas, K.A., A. Kiourti, and K.S. Nikita. *Biocompatibility of implantable antennas: Design and performance considerations*. in *The 8th European conference on antennas and propagation (EuCAP 2014)*. 2014. IEEE.
29. Ullah, S., et al., *A review of wireless body area networks for medical applications*. arXiv preprint arXiv:1001.0831, 2010.
30. Kishk, A., *Advancement in microstrip antennas with recent applications*. 2013: BoD—Books on Demand.
31. Islam, M.N. and M.R. Yuce, *Review of medical implant communication system (MICS) band and network*. Ict Express, 2016. **2**(4): p. 188-194.
32. Islam, M.R., et al. *Design of a passive RFID tag antenna at 2.45 GHz for mounting on various platforms*. in *2011 IEEE International RF & Microwave Conference*. 2011. IEEE.
33. Rahmat-Samii, Y. and L. Song, *Advances in Communication and Biomedical Antenna Developments at the UCLA Antenna Lab: Handheld, Wearable, Ingestible, and Implantable [Bioelectromagnetics]*. IEEE Antennas and Propagation Magazine, 2021. **63**(5): p. 102-115.
34. Bhalla, R., *Analysis of broadband and dual band microstrip patch antennas*. 2001.